Efficient Receiver Design for Cooperative Wireless Networks over Fading Channels

Lina Bariah

Nov, 2014

KHALIFA UNIVERSITY

A thesis submitted to Khalifa University of Science, Technology and Research in accordance with the requirements of the degree of M.Sc. by Research in the Department of Electrical and Computer Engineering

Efficient Receiver Design for Cooperative Wireless Networks over Fading Channels

by

Lina Bariah

A thesis submitted in partial fulfillment of the
requirements for the degree of

Master of Science by Research in Engineering
(Electrical & Computer Engineering)

at

Khalifa University

Thesis Committee

Dr. Sami Muhaidat (Supervisor)
Khalifa University

Prof. Mohamed-Slim Alouini, (External Examiner&Committee Chair),
King Abdullah University of Science & Technology, Saudi Arabia

Dr. Arafat Al-Dweik (Co-Supervisor)
Khalifa University

Dr. Shihab Jimaa (Internal Examiner)
Khalifa University

November, 2014

Abstract

Cooperative transmissions exploit the benefits of Multiple-Input Multiple-Output (MIMO) antennas, by creating virtual antenna arrays to provide spatial diversity and multiplexing gains. Some major challenges in cooperative systems are the time varying nature and the frequency selectivity of cooperative links, which lead to severe Error Rate performance degradation. In this thesis, we first study the multicarrier cooperative transmissions over doubly selective channels. We introduce a novel receiver that enhances the Bit Error Rate (BER) performance of a cooperative system with Space-Frequency Block Coding (SFBC) and Orthogonal Frequency Division Multiplexing (OFDM). We demonstrate that the proposed receiver eliminates the Inter-Carrier Interference (ICI) terms and as a result it reduces the BER error floor caused by the difference in frequency response of the channel over two adjacent subcarriers. Second, given the same cooperative scenario, we present a source precoder design and a relay antenna selection scheme by exploiting the sparsity of the relay gain vector with imperfect channel estimation and spatially correlated antennas at all nodes. For the precoder design, we present a technique which diagonalizes the Mean Squared Error (MSE) matrix to introduce an optimal source precoder design, which aims to minimize the MSE. Extensive Monte Carlo simulation results demonstrate that the performance gain of our proposed schemes over the existing schemes is significant. The simulation results for the proposed schemes show that, considering spatially correlated antennas at all nodes, the proposed model outperforms the other models, even when the antennas are highly correlated.

Declaration

I declare that the work in this thesis was carried out in accordance with the regulations of Khalifa University of Science, Technology and Research. The work is entirely my own except where indicated by special reference in the text. Any views expressed in the thesis are those of the author and in no way represent those of Khalifa University of Science, Technology and Research. No part of the thesis has been presented to any other university for any degree

Signed:
Date:

Acknowledgement

This thesis cannot be completed without thanking all the people who supported and helped me during my masters journey.

First of all, I would express my love and thanks to my parents. I am indebted for my loved mum and dad for their support throughout entire process, I will be grateful forever for their love and guidance, not only on my study but on my full life.

Also, I would express my heartfelt thanks to my beloved husband Rami who was always there cheering me up, stood by me through the good and bad times and for always showing how proud he is of me. His love, patience and encouragement were the main motivations behind completing my masters in a perfect way. Words cannot express how grateful I am to him for all of the sacrifices that he has made on my behalf.

I would like to express my deepest appreciation to my supervisors Dr. Sami Muhaidat and Dr. Arafat Al-Dweik for their guidance and continuous advices and encouragement. Their support, comments and remarks during my masters study have been priceless, my masters journey would not be done perfectly without their great help. Simply, I could not wish for better and friendlier supervisors. Also, a special appreciation and thanks go to Prof. Mahmoud Al-Qutayri who was a teacher, supporter, a guide and a friend during my master study, his motivations and guidance encouraged me to apply for the PhD program. Moreover, sincere thanks go to the external examiner Prof. Mohamed-Slim Alouini and the internal examiner Dr. Shihab Jimaa for their encouragement, questions and insightful comments.

Finally, I would like to thank all my friends for their love, kindness, help and support. A special warm thank goes for my friend Raghad for being with me all the time and for her continuous motivations.

The last word goes for the light of my life Ahmad, my baby boy, who has given me an extra strength to complete the years of my masters by his innocent and love. This thesis is dedicated to him.

Contents

List of Figures

List of Tables

Notations

$(\cdot)^*$	Complex conjugate operation
$(\cdot)^H$	Hermitian transposition operation
$(\cdot)^T$	Transposition operation
$E\{\cdot\}$	Statistical expectation
$(\mathbf{A})^{-1}$	Inverse operation of matrix $\mathbf{A}$
$vec\{\mathbf{A}\}$	Vectorization of matrix $\mathbf{A}$
$\|\mathbf{A}\|_F$	Frobenius norm of matrix $\mathbf{A}$
$tr\{\mathbf{A}\}$	Trace operator of matrix $\mathbf{A}$
$A \to B$	Link between terminal A and terminal B
$\mathbf{I}_N$	$N \times N$ identity matrix
$\|\cdot\|$	Euclidean norm of a vector
$\bigotimes$	Kronecker product
$diag(\cdot)$	The diagonal of a matrix

Chapter 1

Introduction

The next generation wireless networks are expected to support data rates higher than 100 Mbit/s for high mobility users and exceed 1 Gbit/s for low mobility users. Unfortunately, the envisioned high data rates are not feasible with the conventional systems, even with the recent advances in antenna technologies, e.g., multiple-input-multiple-output (MIMO) and smart antennas. Furthermore, under certain conditions, e.g., limited frequency resources and blind spots in the existing cellular networks, the conventional approach in infrastructure-based networks is to increase the density of base stations (BSs), which is inefficient due to the high deployment cost. Therefore, the integration of the so-called multihop relaying, which has been traditionally studied in the context of ad hoc and peer-to-peer networks, into cellular wireless networks is considered to be the most feasible solution to facilitate almost ubiquitous high data rate coverage effectively [1][2].

There have been recent growing interests in both academia and industry in integrating multihop relaying into the next generation infrastructure-based networks such as LTE-Advanced, 802.11s, and 802.16j (WiMax) networks [3][4]. Multihop communications can be realized through the use of low-power, low-cost relays or through other wireless terminals in the network. Information in multihop communications is passed between two terminals (nodes) over multihop transmission.

Recently, a variant of multihop relaying known as cooperative diversity or relay-assisted networks has emerged, generally it is used in infrastructure-less based networks [5] as a promising way to increase spectral and power efficiency, network coverage, and reduce outage probability. Similar to multi-antenna transceivers, relays provide diversity by creating multiple replicas of the signal of interest. The basic idea behind relay-assisted networks is that various terminals/nodes in a relay network attempt to assist each other in moving information around the network, instead of competing for system resources. The result is an improvement of the overall quality of services (such as the statistical measures of bit-error-rate, outage, throughput, and delay) at all the nodes and an associated increase in system spectral. This research focuses on studying the main aspects of the cooperative systems and the main challenges that faces the cooperative systems and it provides solutions for some of these challenges.

1.1 Motivations and Problem Statement

An attractive feature of the cooperative transmission is that it could be combined with other diversity schemes like the Space-Time Block Coding (STBC) and Space-Frequency Block Coding (SFBC) to provide better performance. In some applications, using STBC system in combination with cooperative transmission adds valuable performance enhancement, and this is driven by its ability to provide high data rate and full diversity [6]. However, a main drawbcak of the cooperative STBC systems is its sensitivity to channel time variations which destroys the orthognality of one codeword. Moreover, when an OFDM system is considered with cooperative STBC systems, channel variations cause Inter-Carrier Interference (ICI) between the adjacent subcarriers [7].

In this thesis, we present a cooperative SFBC-OFDM system, where data is transmitted over multiple adjacent subcarriers instead of multiple time slots. In severe frequency selective channels, where channels are varying over adjacent subcarriers, the performance of cooperative SFBC-OFDM system is subject to high degradation. The main focus of this research is to provide some solutions for cooperative SFBC-OFDM systems in real scenarios, especially the effect of the frequency selectivity of the wireless channels. Moreover, we aim to enhance the performance of MIMO cooperative systems in practical scenarios, through minimizing the MSE for spatially correlated antennas and imperfect Channel State Information (CSI).

1.2 Objectives

The main objectives of this thesis can be summarized as follows:

- Provide a technique for doubly selective channels for a cooperative SFBC-OFDM system. The targeted technique should be efficient for different fading scenarios where channels experience different delay spreads and gains.

- Provide a technique for AF Cooperative MIMO systems with taking into consideration practical scenarios, where imperfect CSI and spatially correlated antennas are considered.

1.3 Thesis Contributions

The main contributions of this thesis are twofold. First, we focus on providing efficient techniques to enhance the BER performance of Cooperative SFBC-OFDM system in doubly selective channels. Second, we address the problem of precoding design and antenna selection in MIMO cooperative system assuming practical scenarios.

1.3.1 Cooperative SFBC-OFDM System

Recently, it has been shown that cooperative STBC-OFDM system performs efficiently over static multipath fading channels, while the performance suffers from high degradation over time varying channels. Cooperative SFBC-OFDM systems are introduced to solve the problem of channel time variations, where data is transmitted over multiple adjacent subcarriers. It has been demonstrated that the performance of cooperative SFBC-OFDM systems is robust over time varying channels. However, in severe frequency selective channels, where channels are varying over adjacent subcarriers, the performance of cooperative SFBC-OFDM systems is susceptible to high degradation.

A main contribution of this thesis is to introduce a new receiver design for cooperative SFBC-OFDM system with two transmit antennas and one receive antenna to tackle the effect of doubly selective channels. The proposed receiver is based on avoiding the matrix inversion of the classical Zero Forcing (ZF) receivers while maintaining similar diversity gain as the Matched Filter (MF) receivers, which are known to lead to error floor. Extensive Monte-Carlo simulations are conducted to evaluate the performance of the proposed model over different channel scenarios. The simulation results show that the BER of the proposed model outperforms the BER performance of the cooperative SFBC-OFDM and cooperative STBC-OFDM system over doubly selective channels, and this means that the proposed receiver efficiently mitigates the effect of channel time variations and frequency selectivity.

1.3.2 MIMO Cooperative System

MIMO cooperative systems are considered one of the main key for future wireless transmissions, due to the fact that they can provide high spectral efficiency and link reliability. However, space limitations in some MIMO cooperative applications lead to interference between the antennas and as a consequence the performance of MIMO cooperative systems suffers form high degradations.

Another main focus of this thesis is to provide an optimal precoder design and relay antenna selection scheme under sparse signal constraints to provide better performance of a MIMO cooperative system. We emphasize the need to consider practical scenarios by including imperfect CSI and spatially correlated antennas in the proposed model. For an optimal precoder design, considering the MMSE criterion, a power constrained optimization problem is solved using the Singular Value Decomposition (SVD) and the Generalized SVD (GSVD) of the channels matrices. Orthogonal Matching Pursuit (OMP) algorithm is adopted for the design of the gain control matrix at the relay, where the OMP algorithm iteratively locates one locally optimum solution by solving one least square problem. The located solution at each iteration is considered as one optimum selection of the sparsely structured gain vector. Monte-Carlo simulations are carried out to assess the performance of the proposed model under various antenna correlation factors and different channel estimation errors. As a benchmark, simulation results of a joint source/relay precoders, in which the SVD of the channel matrices are used to minimize the MSE, is considered for evaluation and comparison purposes. Simulation results demonstrates that the performance gain of the proposed model over the benchmark scheme is significant.

1.4 Outline of the Thesis

This thesis is organized as follows:

Chapter 2 represents a literature review and background about MIMO and cooperative systems. An overview about the MIMO systems, their main aspects and their main problems are discussed and a detailed description about the MIMO OFDM systems is provided. Also, an overview about the cooperative systems is introduced in addition to a discussion about the cooperative protocol and relaying modes. Simulation results are provided to assess the performance of the MIMO and cooperative systems.

In Chapter 3 a novel receiver design for cooperative SFBC-OFDM system is introduced. The chapter started by stating the problem behind the proposed model and the adopted system model is mentioned. A detailed design for the receiver is provided and simulation results are used to evaluate the performance of the proposed model.

In Chapter 4 we propose an optimal source precoder design with antenna selection scheme at the relay for AF MIMO cooperative network and channel estimation. The problem statement of the proposed model is defined then a detailed system model is introduced in addition to the channel correlation model and the imperfect channel estimation modeling. Intensive discussion regarding the proposed source precoder design is provided in Section 4.3 and Section 4.4 provides a detailed design for the antennas selection technique. A benchmark model is provided for evaluation and comparison purposes. Simulation results are provided for performance assessment.

Chapter 2

Background

In this chapter, we cover the background material and establish the models that will be used throughout this thesis. First, we present an overview of MIMO systems. Then, we discuss the performance of the STBC-OFDM and SFBC-OFDM systems. We next present an overview of cooperative communications, its main aspects, the value that is added by considering the cooperative transmission and the challenges that face cooperative systems.

2.1 Multiple-Input Multiple-Output (MIMO) Systems

2.1.1 Overview of MIMO Systems

Multiple-Input Multiple-Output (MIMO) systems consist of multiple antennas at the transmitter and the receiver ends. MIMO systems have been widely considered to improve the performance of the wireless systems in fading environment and improve data rates. MIMO systems operate in two modes, i.e., multiplexing and diversity modes. Multiplexing mode is a transmission technique for MIMO systems where multiple separately-encoded data streams are transmitted through multiple antennas independently. MIMO multiplexing technique helps to enhance the system's capacity and it can increase data throughput approximately linearly with the number of antennas. In spatial multiplexing, multiple independent data streams are transmitted in parallel over multiple independent fading channels [8][9]. IEEE 802.16e and IEEE 802.11n with up to 4 spatial multiplexed data streams are main applications for MIMO spatial multiplexing [10]. However, when applying spatial multiplexing to MIMO systems, the parallel transmission of multiple signals streams leads to interferences between the signals streams [11]. Meanwhile, diversity mode is used to establish high quality links by the deployment of multiple antennas at the transmitter to send redundant replicas of the transmitted data over multiple independent fading channels, which enhances the transmission reliability while maintaining bandwidth and power efficiency [12–14]. Space-Time Coding (STC) is one of the proposed techniques to realize MIMO diversity. Schematic representation of a MIMO system is represented in Fig. (2.1).

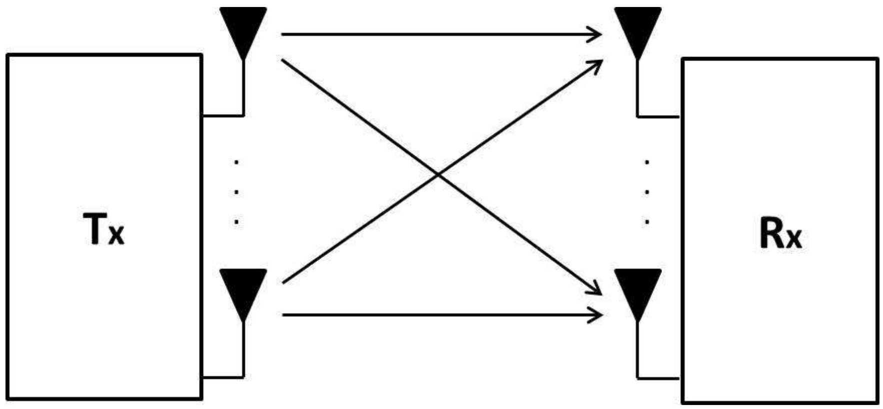

Figure 2.1: Schematic representation of MIMO system

Channel model of MIMO system:
Considering a MIMO system with number of antennas N_T and N_R at the transmitter and the receiver, respectively, the received signal at the receiver end can be expressed as

$$\mathbf{y} = \mathbf{H}\mathbf{a} + \mathbf{n}, \tag{2.1}$$

where $\mathbf{a} = \left[a_0, a_1, a_2, \cdots, a_{(N_T-1)}\right]^T$ is the transmitted vector of size N_T, $\mathbf{n}$ is additive white Gaussian noise with zero mean and variance σ_n^2 and $\mathbf{H}$ is the $N_R \times N_T$ channel matrix between the transmitter and the receiver. $\mathbf{H}$ can be expressed as

$$\mathbf{H} = \begin{bmatrix} h_{0,0} & h_{0,1} & \cdots & h_{0,N_T-1} \\ h_{1,0} & h_{1,1} & \cdots & h_{1,N_T-1} \\ \vdots & \ddots & \ddots & \vdots \\ h_{N_R-1,0} & h_{N_R-1,1} & \cdots & h_{N_R-1,N_T-1} \end{bmatrix}, \tag{2.2}$$

where $h_{m,n}$ are the channel frequency response from antenna n at the transmitter to antenna m at the receiver. At the receiver side, different known decoders can be used to extract the transmitted data from the received signal:

- Zero forcing (ZF) decoder and can be expressed as [15]

$$\mathbf{G}_{zf} = \left(\mathbf{H}^H\mathbf{H}\right)^{-1}\mathbf{H}^H. \tag{2.3}$$

The received signal after using the ZF receiver can be expressed as

$$\hat{\mathbf{a}}_{ZF} = \mathbf{a} + \underbrace{\left(\mathbf{H}^H\mathbf{H}\right)^{-1}\mathbf{H}^H\mathbf{n}}_{\text{amplified noise}}, \tag{2.4}$$

where $\mathbf{a}$ is the transmitted data stream, $\mathbf{n}$ is AWGN with zero mean and variance σ_n^2.

- Minimum Mean Squared Error (MMSE) decoder and can be expressed as [16]

$$\mathbf{G}_{mmse} = \mathbf{H}^H\left(\mathbf{H}\mathbf{H}^H + \sigma_n^2\mathbf{I}_{N_T}\right)^{-1}. \tag{2.5}$$

The received signal after using the ZF receiver can be expressed as

$$\hat{\mathbf{a}}_{MMSE} = \mathbf{G}_{mmse}\mathbf{y}, \tag{2.6}$$

MMSE receivers are widely considered due to their enhanced performance compared to the ZF receivers. Also, MMSE receivers enjoy a low complexity implementation.

- Maximum-likelihood (ML) decoder and the decoded codewords using the ML decoder can be expressed as [17]

$$\hat{\mathbf{a}}_{ML} = arg\ min\left\|\mathbf{y} - \mathbf{H}\mathbf{a}\right\|^2 \tag{2.7}$$

2.1.2 MIMO Orthogonal Frequency Division Multiplexing

Orthogonal Frequency Division Multiplexing (OFDM) is a transmission technology that is introduced to overcome the problem of the inter-symbol interference (ISI) in a multicarrier wireless transmission by converting the frequency selective channel into multiple narrowband parallel flat fading channels [18]. OFDM technology is considered as an efficient technique to achieve similar data rate as the single carrier transmission but with providing high spectral efficiency, by allowing the spectrum of individual subcarriers to overlap without interference because of the orthogonality between the subcarriers [19][20], as shown in Fig. (2.2).

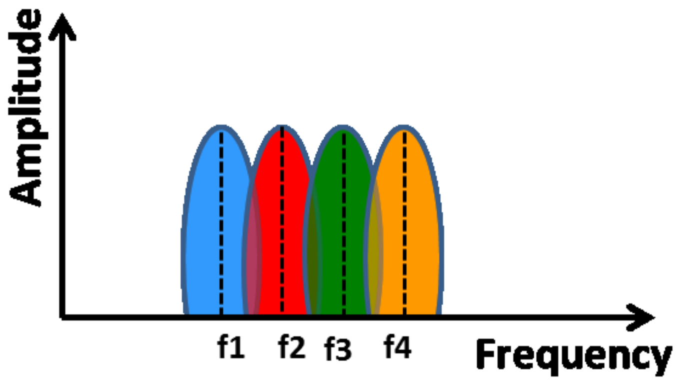

Figure 2.2: OFDM spectrum

A general OFDM block diagram is shown in Fig. (2.3). At the transmitter side, transmitted data stream is converted into parallel multiple substreams by using the serial to parallel converter and then the signal is OFDM modulated by applying N-point Inverse Fast Fourier transform (N-IFFT). Cyclic prefix (CP) symbols are then inserted to maintain the orthogonality between subcarriers even in a time dispersive channels to avoid the ISI. After CP removal at the receiver side, N-point Fast Fourier Transform (N-FFT) is applied to convert the signal from time domain to frequency domain [21]. At the end, the multiple substreams are converted back to one main stream using parallel to serial converter.

Considering N subcarriers, the output of the IFFT process is

$$\mathbf{x} = \mathbf{F}^H \mathbf{a}, \tag{2.8}$$

where $\mathbf{a}$ is the transmitted signal and $\mathbf{F}^H$ is the hermitian transpose of the $N \times N$ FFT matrix $\mathbf{F}$. CP of size P is inserted to the preamble of the OFDM symbol to form a new symbol of length $N_a = N + P$. At the receiver side, after the removal of the CP, the output of the FFT process is

$$\tilde{\mathbf{r}} = \mathbf{F}\mathbf{H}\mathbf{F}^H \mathbf{a} + \mathbf{F}\mathbf{n}, \tag{2.9}$$

where $\mathbf{H}$ is the channel matrix and $\mathbf{n}$ is additive white Gaussian noise with zero mean and variance $\mathcal{N} \sim (\mu, \sigma_n^2)$ [22].

Despite the effectiveness of the OFDM technology in the frequency selective channels, OFDM is very sensitive to time and frequency synchronization errors. Changes in frequency and time offsets lead to orthogonality loss between the overlapped subcarriers and as a result this will cause ICI between subcarriers and performance degradation [23].

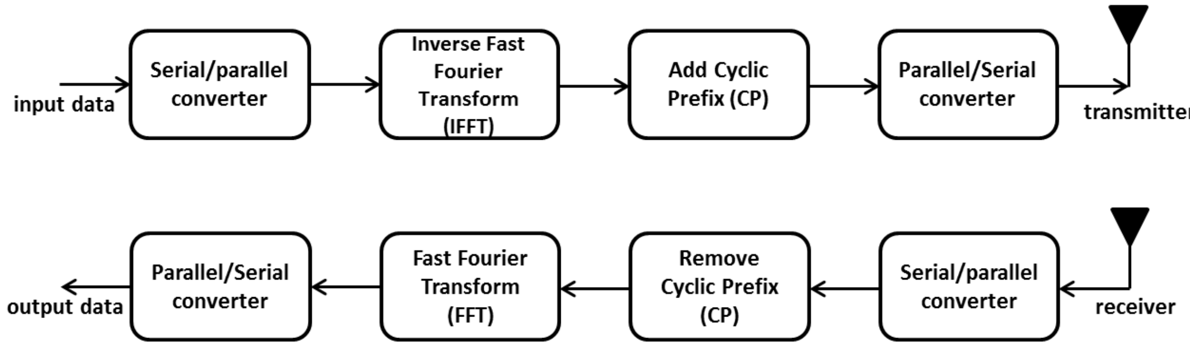

Figure 2.3: OFDM block diagram

2.1.3 Space-Time Block Coding OFDM

Space-Time Block Coding (STBC) is a low complexity encoding method that exploits transmit diversity to provide diversity gain, high codeword and better system's performance [24]. STBC in combination with OFDM reduces fading effect by the deployment of the transmit diversity in frequency selective channels. Alamouti [25] introduced the well-known STBC scheme that considers two transmit antennas to transmit two symbols over two time slots. In Alamouti transmission scheme, the first antenna transmits a_1 and the second antenna transmits a_2 during the first time slot. In the second time slot, the first antenna transmits $-a_2^*$ and the second antenna transmits a_1^*, as presented in Table (2.1).

Table 2.1: Space-time diversity scheme of Alamouti

space ↓	time	
	t_1	t_2
T_{x1}	a_1	$-a_2^*$
T_{x2}	a_2	a_1^*

STBC-OFDM system model:

Considering two transmit antennas and one receive antenna, $\mathbf{a_1}$ and $\mathbf{a_2}$ are two data streams to be transmitted using STBC-OFDM transmission technique. First, the two data streams are OFDM modulated using N-point IFFT as follows

$$\mathbf{x}_1 = \mathbf{F}^H \mathbf{a}_1 \tag{2.10}$$

and

$$\mathbf{x}_2 = \mathbf{F}^H \mathbf{a}_2, \tag{2.11}$$

where $\mathbf{F}^H$ is the hermitian transpose of the normalized N-FFT matrix $\mathbf{F}$. The nth sample of the two sequences $\mathbf{x}_1$ and $\mathbf{x}_2$ can be expressed as

$$x_{1,n} = \frac{1}{\sqrt{N}} \sum_{k=0}^{N-1} a_{1,k}\, e^{i2\pi n \frac{k}{N}}, \quad n = 0, 1, \cdots, N-1 \tag{2.12}$$

and

$$x_{2,n} = \frac{1}{\sqrt{N}} \sum_{k=0}^{N-1} a_{2,k}\, e^{i2\pi n \frac{k}{N}}, \quad n = 0, 1, \cdots, N-1. \tag{2.13}$$

A CP of size P is added by inserting a copy of the last P samples of the OFDM modulated signal at the preamble of it to achieve an OFDM symbol of size $N_a = N + P$. It is worth noting that the size of the CP samples should be equal to or larger than the channel delay spread in multipath propagation environment to avoid interblock interference and to help maintaining the orthogonality between the OFDM subcarriers [26].

Quasi-static multipath channels are considered, where the channels are constant over one OFDM symbol and are slowly varying over two consecutive OFDM symbols [27][28]. The channel consists of $(L_h + 1)$ independent multipath components, each of which has a delay spread $m \times T_s$ and path gain h_m, where T_s is the receiver sampling time and $m \in \{0, 1, \cdots, L_h\}$. During the first time slot, the received signal at the receiver end after the CP removal is

$$\mathbf{y}^1 = \mathbb{H}^{1,1}\mathbf{x}_1 + \mathbb{H}^{2,1}\mathbf{x}_2 + \mathbf{z}_1, \tag{2.14}$$

where $\mathbf{y}^\tau$ is the received signal during time slot $\tau = 1$ and $\mathbb{H}^{\omega,\tau}$ is an $N \times N$ circulant channel matrix between the receiver and transmit antenna ω during time slot $\tau = 1$, $\omega \in \{1, 2\}$. $\mathbf{z}_\tau$ is an additive white Gaussian noise (AWGN) with zero mean and variance $\sigma_z^2 = E\left(|z_{n1}|\right)$ during time slot $\tau = 1$. $\mathbb{H}^{\omega,\tau}$ can be expressed as [29]

$$\mathbb{H}^{\omega,\tau} = \begin{bmatrix} h_0^{\omega,\tau} & 0 & \cdots & 0 & h_{L_h}^{\omega,\tau} & \cdots & h_1^{\omega,\tau} \\ h_1^{\omega,\tau} & \ddots & & & & \ddots & \vdots \\ \vdots & & \ddots & & & & h_{L_h}^{\omega,\tau} \\ h_{L_h}^{\omega,\tau} & & & \ddots & & & 0 \\ 0 & \ddots & & & \ddots & & \vdots \\ \vdots & \ddots & \ddots & & & \ddots & 0 \\ 0 & \cdots & 0 & h_{L_h}^{\omega,\tau} & \cdots & h_1^{\omega,\tau} & h_0^{\omega,\tau} \end{bmatrix}, \tag{2.15}$$

where $h_m^{\omega,\tau}$ is the mth path channel gain from transmit antenna ω and at time period τ. Hence, the FFT of the received signal can be calculated as

$$\begin{aligned} \mathbf{r}^1 &= \mathbf{F}\mathbf{y}^1 \\ &= \mathbf{F}\mathbb{H}^{1,1}\mathbf{x}_1 + \mathbf{F}\mathbb{H}^{2,1}\mathbf{x}_2 + \mathbf{F}\mathbf{z}_1 \\ &= \mathbf{F}\mathbb{H}^{1,1}\mathbf{F}^H\mathbf{a}_1 + \mathbf{F}\mathbb{H}^{2,1}\mathbf{F}^H\mathbf{a}_2 + \mathbf{F}\mathbf{z}_1. \end{aligned} \tag{2.16}$$

Considering that $\mathbf{F}^{-1} = \mathbf{F}^H$ because $\mathbf{F}$ is a unitary matrix, the channel matrix $\mathbb{H}^{\omega,\tau}$ can be diagonalized by the FFT matrix $\mathbf{F}$ and the IFFT matrix $\mathbf{F}^H$ as

$$\begin{aligned} \bar{\mathbf{H}}^{\omega,\tau} &= \mathbf{F}\mathbb{H}^{\omega,\tau}\mathbf{F}^H \\ &= diag\left(\left[H_0^{\omega,\tau}, H_1^{\omega,\tau}, \cdots, H_{N-1}^{\omega,\tau}\right]\right), \end{aligned} \tag{2.17}$$

where $H_k^{\omega,\tau}$ is the channel frequency response at subcarrier k in frequency domain from antenna ω, in time slot τ. Therefore, the received kth sample in the first time slot can be expressed as follows

$$r_k^1 = H_k^{1,\tau}\, a_{1,k} + H_k^{2,\tau}\, a_{2,k} + \eta_1^k, \tag{2.18}$$

where r_k^τ is the kth received sample during time slot $\tau = 1$, η_1^k is the FFT of the kth complex random noise sample in the first time slot. In the second time slot, the first antenna transmits $-\mathbf{a}_2^*$ and the second antenna transmits $\mathbf{a}_1^*$. Similarly, the received kth sample at the second time slot is

$$r_k^2 = -H_k^{1,\tau}\, a_{2,k}^* + H_k^{2,\tau}\, a_{1,k}^* + \eta_2^k. \tag{2.19}$$

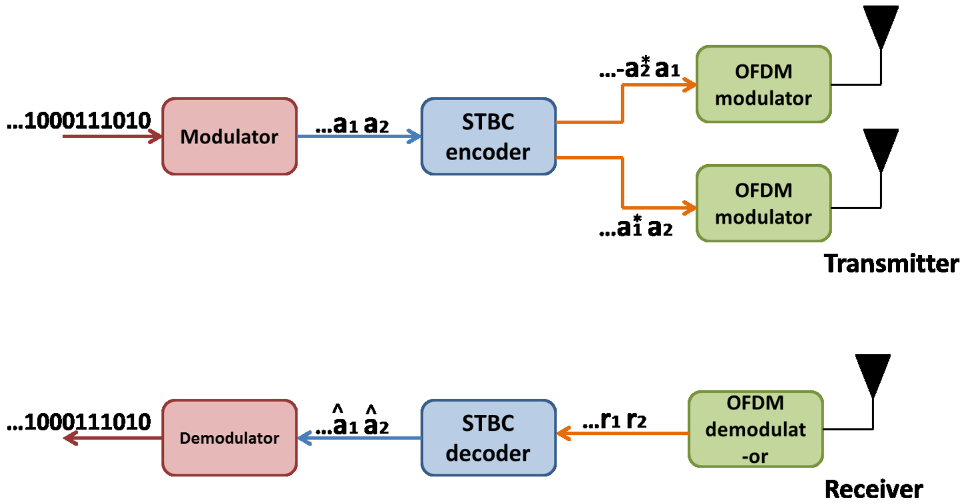

Figure 2.4: STBC-OFDM block diagram

The received signal at the first and second time slots can be equivalently expressed in matrix form as

$$\begin{bmatrix} r_k^1 \\ (r_k^2)^* \end{bmatrix} = \begin{bmatrix} H_k^{1,\tau} & H_k^{2,\tau} \\ \left(H_k^{2,\tau}\right)^* & \left(-H_k^{1,\tau}\right)^* \end{bmatrix} \begin{bmatrix} a_1 \\ a_2 \end{bmatrix} + \begin{bmatrix} \eta^1 \\ (\eta^2)^* \end{bmatrix}. \tag{2.20}$$

Eqn. (2.20) can be written in compact form as

$$\mathbf{r} = \mathbf{H}\mathbf{a} + \boldsymbol{\eta}. \tag{2.21}$$

Since we are considering quasi-static channel, the channel is assumed static over multiple time slots and therefore we can drop the time symbol τ from the channel matrix,

$$\mathbf{H} = \begin{bmatrix} H_k^1 & H_k^2 \\ (H_k^2)^* & (-H_k^1)^* \end{bmatrix}. \tag{2.22}$$

Finally, STBC decoder is used to process, decode and combine the received samples. The output of the decoder can be expressed as

$$\begin{aligned} \hat{\mathbf{s}} &= \mathbf{H}^H \mathbf{r} \\ &= \mathbf{H}^H \mathbf{H}\mathbf{a} + \mathbf{H}^H \boldsymbol{\eta}, \end{aligned} \tag{2.23}$$

where $\mathbf{H}^H$ is the Hermitian transpose of the channel matrix $\mathbf{H}$. The decoded symbols $\hat{s}_1$

and $\hat{s}_2$ are applied to a detector to detect the transmitted symbols $\hat{a}_1$ and $\hat{a}_2$ [30–33]. BER performance of 2×1 STBC-OFDM system with considering that transmitted data is chosen randomly from BPSK constellation is [34]

$$P_{\text{bpsk}} = \frac{1}{2}\left(1 - \delta \sum_{k=0}^{1} \binom{2k}{k} \left(\frac{1-\delta^2}{4}\right)^k\right), \tag{2.24}$$

where $\delta = \sqrt{\frac{E_b/N_o}{2+E_b/N_o}}$.

2.1.4 Space-Frequency Block Coding OFDM

Space-Frequency Block Coding (SFBC) is a transmission scheme that is used to provide high quality transmission in time varying channel or when the Doppler spread is very high [35]. The basic idea behind SFBC scheme is to transmit data over multiple adjacent subcarriers instead of multiple time slots to combat the effect of time varying channels. For SFBC-OFDM system, to provide better performance, the channel has to be constant over multiple adjacent subcarries during one OFDM symbol. In doubly selective channels, the channel is varying among adjacent subcarriers and consequently SFBC-OFDM system will suffer from ICI which leads to diversity gain loss [36] [37]. Block diagram of an SFBC-OFDM system is shown in Fig. (2.5). Transmitted data stream $\mathbf{a} = [a_0, a_1, \cdots, a_{N-1}]$ of size N is applied to a standard STBC encoder first,

$$a_k \;\; a_{k+1} \rightarrow \begin{bmatrix} a_k & -a_{k+1}^* \\ a_{k+1} & a_k^* \end{bmatrix}, \tag{2.25}$$

where k represents even subcarrier and $k+1$ represents odd subcarrier. The output samples of the STBC encoder are buffered to form two SFBC data symbols,

$$\mathbf{b}_1 = \left[a_0, -a_1^*, a_2, \cdots, a_{N-2}, -a_{N-1}^*\right] \tag{2.26}$$

$$\mathbf{b}_2 = \left[a_1, a_0^*, a_3, a_2^*, \cdots, a_{N-1}, a_{N-2}^*\right]. \tag{2.27}$$

The two streams $\mathbf{b}_1$ and $\mathbf{b}_2$ are OFDM modulated and transmitted through the two antennas. Following the same procedure as in the STBC scheme, the output of the FFT at the receiver is [38][39]

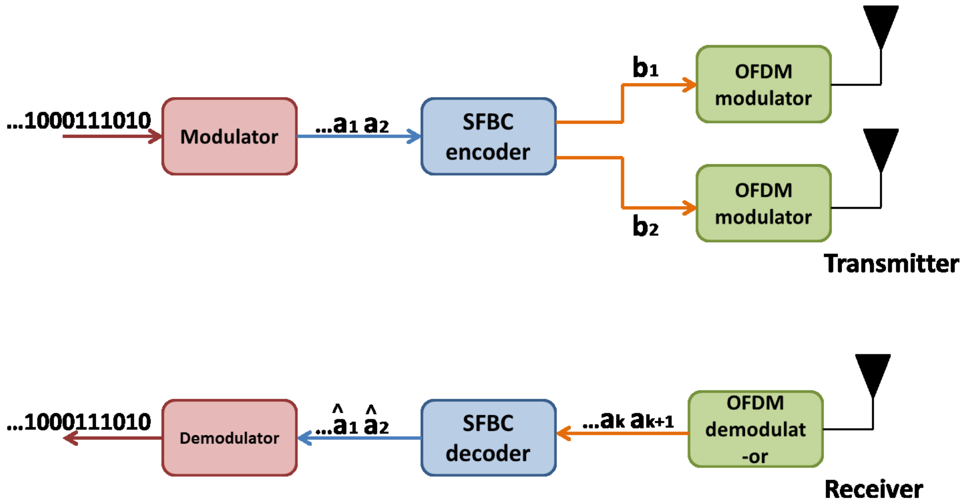

Figure 2.5: SFBC-OFDM block diagram

$$\mathbf{r} = \mathbf{H}^1\mathbf{b}_1 + \mathbf{H}^2\mathbf{b}_2 + \boldsymbol{\eta}, \tag{2.28}$$

where $\boldsymbol{\eta}$ is AWGN vector with zero mean and variance σ_η^2. Considering $\mathbf{H}^\omega$ is diagonal channel matrix between the receiver and antenna ω, $\omega \in \{1, 2\}$,the output of the FFT at subcarrier k and $k+1$ are

$$r_k = H_k^1\, a_k + H_k^2\, a_{k+1} + \eta_k \tag{2.29}$$

and

$$r_{k+1} = -H_{k+1}^1\, a_{k+1}^* + H_{k+1}^2\, a_k^* + \eta_{k+1}, \tag{2.30}$$

where a_k is the kth element of $\mathbf{b}_1$, a_{k+1} is the kth element of $\mathbf{b}_2$, $-a_{k+1}^*$ is the $(k+1)$th element of $\mathbf{b}_1$ and a_k^* is the $(k+1)$th element of $\mathbf{b}_2$.

Since the channel is considered to be constant over at least two adjacent subcarriers, i.e. $H_k = H_{k+1}$, $\mathbf{H}$ can be represented by Eqn.(2.22). Hence, the output of the FFT at subcarrier k and $k+1$ can be represented in matrix form as

$$\begin{bmatrix} r_k \\ r_{k+1}^* \end{bmatrix} = \begin{bmatrix} H_k^1 & H_k^2 \\ (H_k^2)^* & (-H_k^1)^* \end{bmatrix} \begin{bmatrix} a_k \\ a_{k+1} \end{bmatrix} + \begin{bmatrix} \eta_k \\ \eta_{k+1}^* \end{bmatrix}. \tag{2.31}$$

Eqn. 2.31 can be represented in compact form as

$$\mathbf{r} = \mathbf{H}\mathbf{a} + \bar{\boldsymbol{\eta}}. \tag{2.32}$$

The STBC decoder is then used to decode the received signal as follows

$$\hat{\mathbf{s}} = \mathbf{H}^H\mathbf{r} = \mathbf{H}^H\mathbf{H}\mathbf{a} + \mathbf{H}^H\bar{\boldsymbol{\eta}}, \tag{2.33}$$

where $\hat{\mathbf{s}} = \begin{bmatrix} \hat{s}_k \\ \hat{s}_{k+1} \end{bmatrix}$. The decoded symbols $\hat{s}_k$ and $\hat{s}_{k+1}$ are applied to a detector to detect the transmitted symbols $\hat{a}_k$ and $\hat{a}_{k+1}$. The transmission scheme of SFBC-OFDM system is shown in Table. (2.2)

Table 2.2: Space-frequency transmission scheme

space ↓	frequency	
	f_k	f_{k+1}
T_{x1}	a_k	$-a^*_{k+1}$
T_{x2}	a_{k+1}	a^*_k

2.1.5 Simulation Study

This section presents Monte-Carlo simulation results for MIMO-OFDM, STBC-OFDM and SFBC-OFDM systems over static frequency selective channels. The number of carriers $N = 64$ is considered with CP of length $P = 16$. The transmitted data is chosen randomly from BPSK constellation. Three channel models are generated with different number of multipath components, different delay spread and different channel gains. The first channel (Ch. 1) is assumed to have 5 taps ($L_h = 4$) with normalized delay spread vector $[0, 1, 2, 3, 4]$ and gain $[0.35, 0.25, 0.18, 0.13, 0.09]$, where L_h+1 is the number of multipath components. The second channel (Ch. 2) has 5 taps ($L_h = 11$) with normalized delay spread $[0, 1, 2, 6, 11]$ and gain $[0.34, 0.28, 0.23, 0.11, 0.04]$. The last channel (Ch. 3) has 4 taps ($L_h = 12$) with normalized delay spread $[0, 4, 8, 12]$ and gains $[0.25, 0.25, 0.25, 0.25]$ [40]. AWGN is considered with zero mean and variance $\sigma_n^2 = N_o/2$. Fig. (2.6) shows a comparison between the BER performance of the three channel models and the theoretical performance for an OFDM system. As expected, the BER performance over the three models is identical, and this stimulated by the ability of the OFDM technique to convert the frequency selective channels, with different number of multipath components, into parallel flat fading channels. Fig. (2.7) represents the BER performance of STBC-OFDM system with different channel models. From Fig.

(2.7), the BER performance of the STBC-OFDM system is independent of the frequency selectivity of the channels as long as the channels remain constant over multiple time slots, which is the main assumption for the STBC-OFDM system here. Hence, as the number of the multipath component changes, the BER performance of the STBC-OFDM system remains the same. On the other hand, it is noticeable from the BER performance comparison in Fig. (2.8) that the SFBC-OFDM system is affected by the frequency selectivity of the channels and this is because the SFBC-OFDM system depends on transmitting data over multiple adjacent subcarriers. Consequently, for better performance, it is required that the channel should remain constant over at least two adjacent subcarriers. It is observed from Fig. (2.8) that as we increase the number of taps of the channel, the system suffers from performance degradation. A comparison between the performance of the STBC and SFBC is shown in Fig. (2.9). From Fig. (2.9), it is observed that the STBC outperforms the SFBC. The BER of the STBC is 10^{-4} for all channels at SNR = 16 dB, while at the same SNR, the BER of the of the SFBC is 4×10^{-4}, 1.8×10^{-3} and 3×10^{-3} for Ch.1, Ch.2 and Ch.3, respectively.

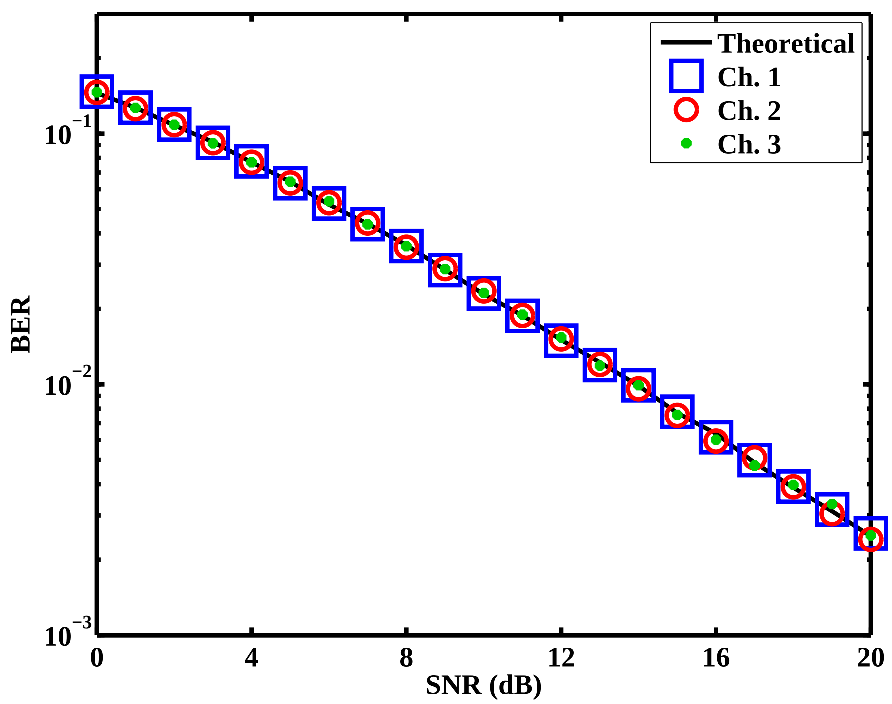

Figure 2.6: BER of OFDM system using BPSK with different channel models

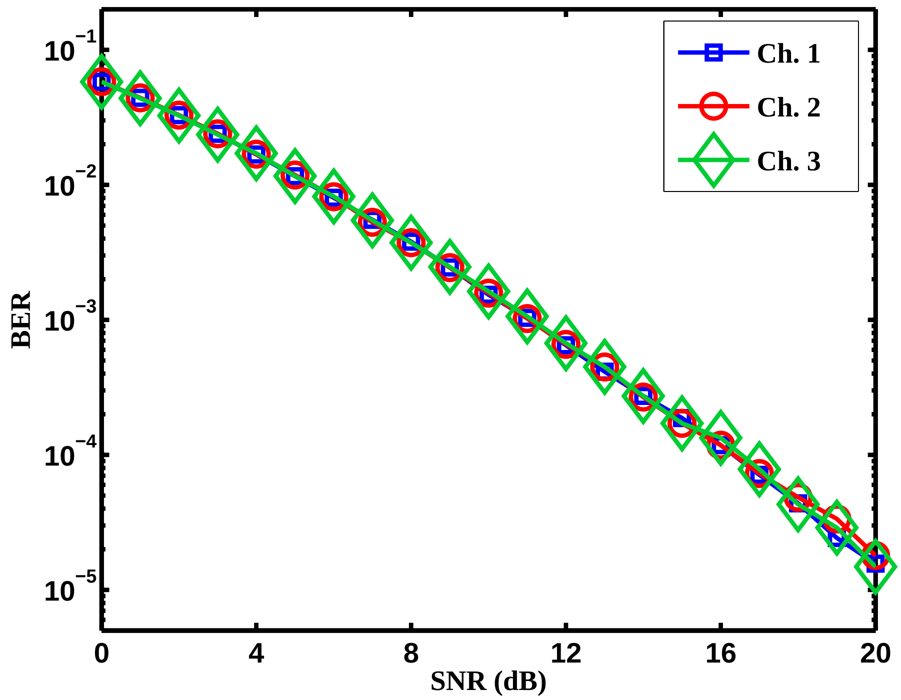

Figure 2.7: BER of STBC for different channel models

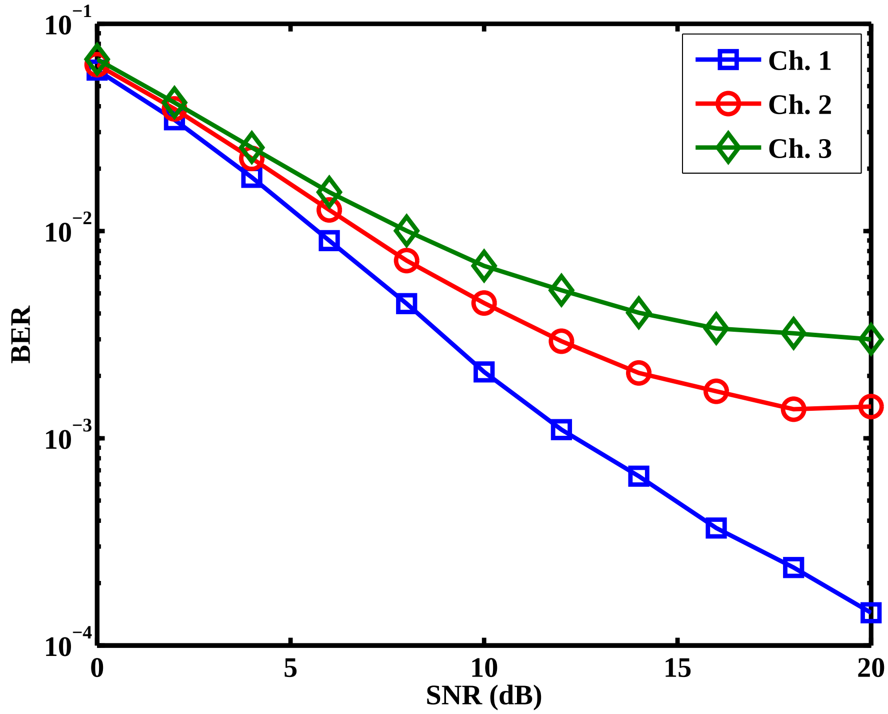

Figure 2.8: BER of SFBC for different channel models

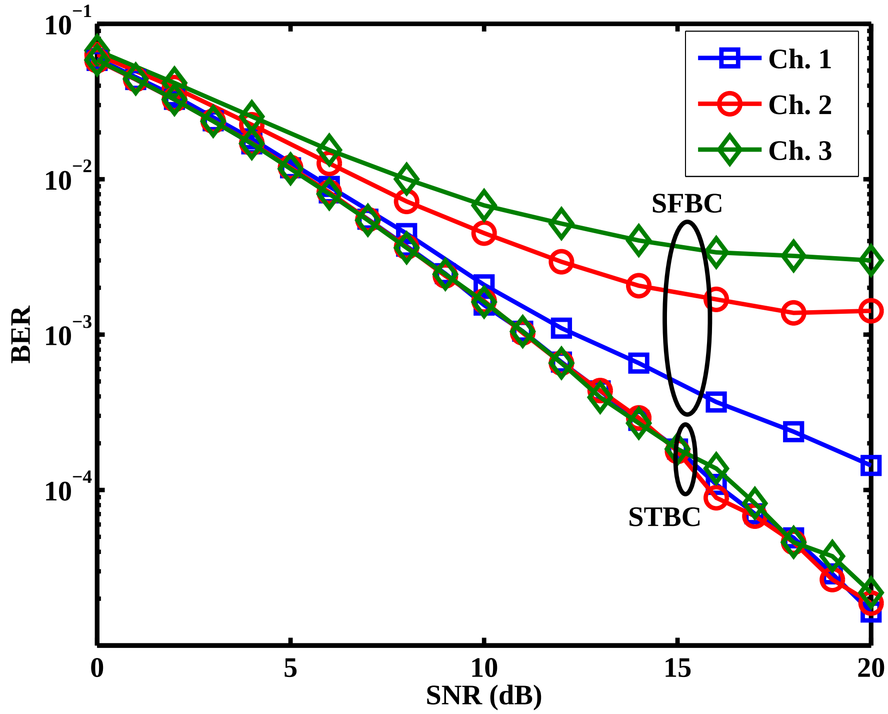

Figure 2.9: BER of STBC and SFBC for different channel models

2.2 Cooperative Communications

2.2.1 Overview of Cooperative Systems

Cooperative communications is a transmission technique that provides spatial diversity in addition to multiplexing gain by utilizing distributed relays to assist data transmission between a source and a destination [41]. Schematic diagram of a cooperative system is shown in Fig. (2.10).

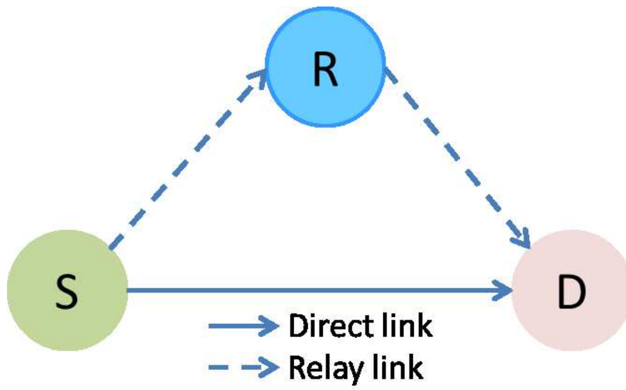

Figure 2.10: Schematic diagram of cooperative system

2.2.2 Cooperative Protocols

Transmission between the three nodes in a cooperative wireless network differs based on the nodes that transmit and the nodes that listens at each time slot. Nabar *et al.* in [42] introduced three cooperative protocols, i.e., Protocol I, Protocol II and Protocol III. In protocol I, in the first time slot, the source communicates with both the relay and the destination. Hence, the received signals at the relay and destination in the first time slot are

$$\mathbf{y}_R^1 = \mathbf{H}_{SR}^1 \mathbf{a}_1 + \mathbf{n}_r^1 \tag{2.34}$$

and

$$\mathbf{y}_D^1 = \mathbf{H}_{SD}^1 \mathbf{a}_1 + \mathbf{n}_d^1, \tag{2.35}$$

respectively. where $\mathbf{H}_{SR}^1$ and $\mathbf{H}_{SD}^1$ represents source-relay channel matrix and source-destination channel matrix, respectively, in the first time slot. $\mathbf{n}_R^1$ and $\mathbf{n}_D^1$ are AWGN at the relay and the destination, respectively, in the first time slot with zero mean and variances σ_r^2 and σ_d^2, respectively, and $\mathbf{a}_1$ is the transmitted data stream in the first time. In the second time slot, both of the source and relay communicate with the destination. The received signal at the destination is

$$\mathbf{y}_D^2 = \mathbf{H}_{SD}^2\mathbf{a}_2 + \mathbf{H}_{RD}^2\mathbf{y}_R^1 + \mathbf{n}_D^2. \tag{2.36}$$

For protocol II, during the first time slot, similar to protocol I, the source transmits data to the relay and destination. However, during the second time slot, the destination only receives data from the relay. The received signal at the relay and destination during the first time slot are similar to Eqn. (2.34) and Eqn. (2.35), respectively. While in the second time slot, the received signal at the destination form the relay is

$$\mathbf{y}_D^2 = \mathbf{H}_{RD}^2\mathbf{y}_R^1 + \mathbf{n}_D^2. \tag{2.37}$$

For protocol III, in the first time slot, the source only transmits its data to the relay, and this because the destination could be engaged in a transmission to another node during this time slot [43]. The received signal in the relay at the first time slot is expressed as in Eqn. (2.34). In the second time slot, the received signal at the destination form the source and the relay is given by Eqn. (2.36). The three protocols provide different degree of broadcasting and receive collision based on the number of nodes that transmit and the number of nodes that receive in each time slot [44]. Degree of broadcasting is determined by the number of nodes listen to the source node simultaneously, however, receive collision is determined by the number of nodes that transmits to the destination simultaneously. Hence, from Table. (2.3), it can be decided that protocol I and protocol II implement maximum degree of broadcasting, while protocol III does not implement any degree of broadcasting. In term of receive collision, protocol I and protocol III only realizes maximum receive collision. It is noteworthy that protocol II is more efficient in term of battery life than protocol I and protocol III when we consider equal transmission power during all time slots, because it stays silent in the second time slot.

2.2.3 Relaying Mode

The received signal at the relay is processed first at the relay before it being forwarded to the destination. Different relaying modes are introduced to specify the signal processing type at the relay, the common ones are amplify-and-forward (AF), decode-and-forward (DF) and compress-and-forward (CF). In AF relaying mode, the relay only amplifies the received signal from the source without any decoding or demodulation and forwards it again to the destination [45]. In the DF mode, the relay first demodulates the received signal, decodes it and then re-encode it again before forwarding it to the destination [46]. CF relaying mode is used when the relay is unable to decode the received signal, hence, the relay demodulates the reveived signal and then it compress the signal and forward it to the destination [47].

2.2.4 Simulations Study

In this section, Monte-Carlo experiments are performed to investigate the performance of a cooperative system with AF relaying mode and protocol III. Single relay scenario is assumed. All three nodes, source, relay and destination are equipped with single antenna and all links are initially assumed frequency selective multipath fading channels. $S \rightarrow D$ and $R \rightarrow D$ links are assumed balanced, i.e., $E_{SD} = E_{RD}$. Fig. (2.11) shows BER performance of a cooperative system with different SNR values of the link $S \rightarrow R$ link. We can see that as the SNR value of the $S \rightarrow R$ decreases for SNR = 30 dB into SNR = 20 dB, the BER performance of the cooperative system degrades and this is because of the amplified noise through $R \rightarrow D$ link which counteracts any increasing in the signal energy. Fig. (2.12) represents a comparison between a case where the $R \rightarrow D$ link is static and when it is fading. It is noticeable that when the $R \rightarrow D$ link becomes fading, the system suffers from performance decay and gain loss.

Table 2.3: Cooperative transmission protocols

Time slot ↓	Protocol		
	Prtotcol I	Protocol II	Protocol III
t_1	$S \rightarrow R, D$	$S \rightarrow R, D$	$S \rightarrow R$
t_2	$S, R \rightarrow D$	$R \rightarrow D$	$S, R \rightarrow D$

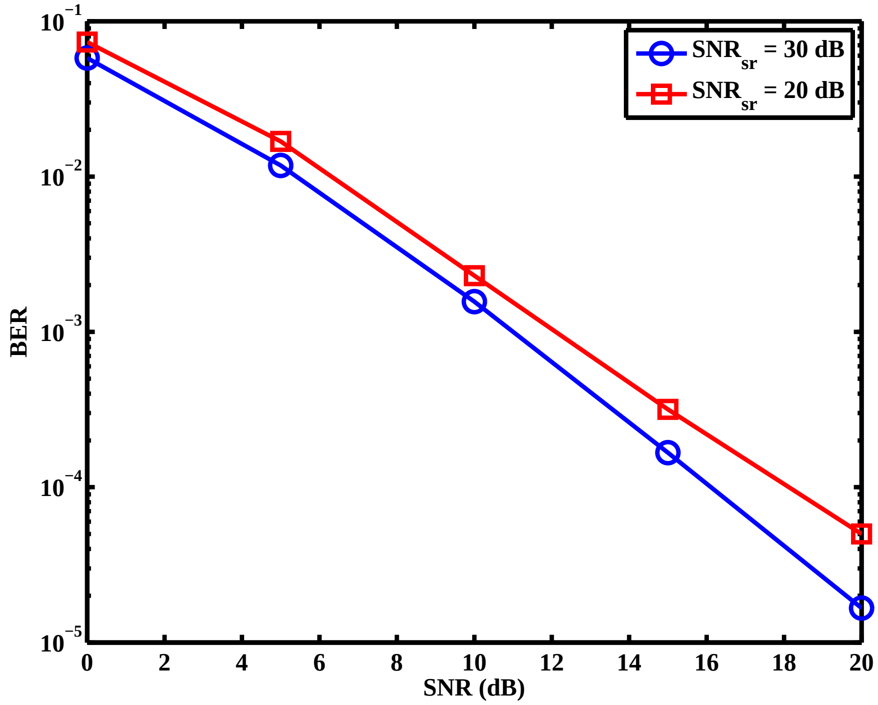

Figure 2.11: BER of cooperative system with different SNR values for S-R link

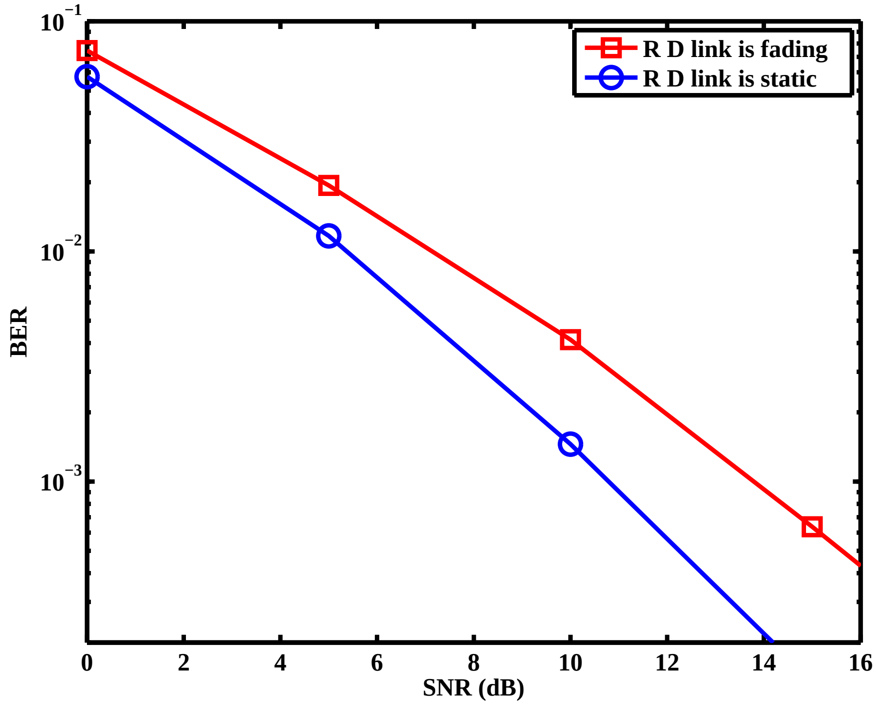

Figure 2.12: BER of cooperative system for static and fading $R \to D$ link

Chapter 3

Receiver Design for Cooperative SFBC-OFDM Over Mobile Channels

In this chapter, we present a novel receiver to enhance the performance and reliability of cooperative SFBC-OFDM systems by minimizing the ICI caused by the variations of the channel frequency responses over multiple adjacent subcarriers.

3.1 Problem Statement

Space-Time Block-Coding (STBC) has been considered recently as an efficient transmit diversity for combating the effect of fading and increasing the transmission reliability. However, STBC is efficient for the case where channels are constant over multiple symbol periods. STBC performance is vulnerable to high performance degradation at high Doppler frequencies. Space-Frequency Block-Coding (SFBC) in combination with OFDM has been considered to minimize the effect of the channel variations, since SFBC data blocks are transmitted over multiple subcarriers [48]. However, in severe frequency-selective channels, the channel coefficients over adjacent subcarriers may vary dramatically. Such variations lead to orthogonality loss and, as a result, Inter-Carrier Interference (ICI) between consecutive subcarriers is introduced. Consequently, the Bit Error Rate (BER) performance of SFBC-OFDM system will suffer from error floor [49]. Ozbek and Ruyet [50] introduce a channel compensation method for a point-to-point SFBC-OFDM system to prevent the error floor caused by the variations of the channel coefficients. They show that SFBC-OFDM system can be used even for channels, where the delay spread is high compared to the symbol duration. Omari et al. [51] propose an enhanced scheme for SFBC-OFDM system. Their proposed scheme utilizes the channel frequency variations in consecutive subcarriers over highly frequency selective channels to adapt the Alamouti decoder to perform higher BER performance. Many other researches have been conducted to improve the performance of the SFBC-OFDM system (see [52–54]). Yao and Dong [55] introduce a low complexity ICI removal technique that enhances the performance of the Cooperative STBC-OFDM system. There have been considerable research efforts on ICI mitigation in Cooperative STBC-OFDM system (see [56–58]). Lu et al. [59] propose an algorithm to mitigate ICI by combining two sets of separately synchronized signal. They utilize the iterative interference cancellation and a maximum-ratio-combining-like technique to further improve the BER performance of cooperative SFBC-OFDM system. Lee et al. [60] adopt the proposed algorithm in [59] and propose a modified version of the receiver structure to enhance the performance.

In this thesis, we design a new receiver for doubly selective channels in cooperative SFBC-OFDM system to mitigate the error floor in the BER performance. The proposed receiver is based on avoiding the matrix inversion operation of the ZF receivers and at the same time it provides diversity gain as the MF receivers, which when used cause an error floor.

3.2 System Model

A cooperative wireless system with a source (S), Relay (R) and Destination (D) terminals is depicted in Fig. 3.1. Data transmission from the source to the destination is assisted by a relay. Cooperative protocol III discussed in Section 2.2.2 is adopted to coordinate the communications process, since we are assuming that the destination could be engaged in another transmission with another network. In protocol III, data transmission passes through two phases, during the first phase, there is no communications between the source and destination. In the second phase, both terminals, source and relay, communicate with the destination through $S \to D$ and $R \to D$ links. All three terminals are equipped with single transmit or receive antenna. We consider that $S \to R$, $R \to D$ and $S \to D$ links are frequency selective multipath fading channels. For $R \to D$ link, AF relaying mode is used, where the relay only amplify the received signal and forward it to the destination.

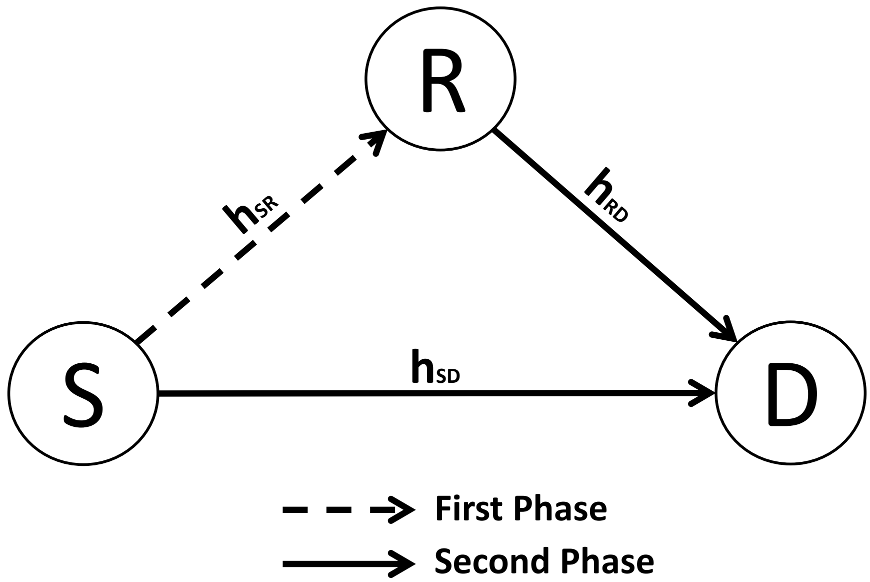

Figure 3.1: Schematic representation of cooperative transmission

For cooperative SFBC system, the first phase is called the OFDM phase, where the data is modulated to form OFDM symbols. The second phase is called the SFBC phase, where the data is coded using SFBC encoder. In OFDM phase, the data sequence $\mathbf{a} = [a_0, a_1, a_2, \cdots, a_{N-1}]$ is split into two sequences each of length $N/2$

$$\mathbf{a}_e = [a_0, a_2, a_4, \cdots, a_{N-2}] \tag{3.1}$$

$$\mathbf{a}_o = [a_1, a_3, a_5, \cdots, a_{N-1}], \tag{3.2}$$

where $\mathbf{a}_e$ and $\mathbf{a}_o$ are the transmitted data at even and odd subcarriers, respectively. The two data sequence, $\mathbf{a}_e$ and $\mathbf{a}_o$, are OFDM modulated by applying N-points Inverse Fast Fourier Transform (IFFT). After that, the OFDM symbols are transmitted from the source to the relay. At the relay terminal, the received signal is

$$\underbrace{\begin{bmatrix} y_R^k \\ y_R^{k+1} \end{bmatrix}}_{\mathbf{y}_R} = \sqrt{E_{SR}}\, \underbrace{\begin{bmatrix} H_{SR}^k & 0 \\ 0 & H_{SR}^{k+1} \end{bmatrix}}_{\mathbf{H}_{SR}} \underbrace{\begin{bmatrix} x_k \\ x_{k+1} \end{bmatrix}}_{\mathbf{x}} + \underbrace{\begin{bmatrix} n_R^k \\ n_R^{k+1} \end{bmatrix}}_{\mathbf{n}_R}, \tag{3.3}$$

where n_R^k and n_R^{k+1} are AWGN samples at subcarriers k and $k+1$, respectively, with zero mean and variance $\sigma_r^2 = N_o/2$. E_{SR} is the energy of the $S \to R$ link, $\mathbf{H}_{SR}$ is the channel matrix between the source and the relay and H_{SR}^k and H_{SR}^{k+1} are the channel responses in frequency domain at even and odd subcarriers, respectively.

Given that the average power of the channel and the transmitted data is normalized to one, the relay normalizes the received signal by the factor $E(|\mathbf{y}_R^2|) = E_{SR} + N_o$ and retransmit it to the destination in the second phase [43]. In SFBC phase, the transmitted signals from the source and the relay are passed through Alamouti SFBC encoder and transmitted over N adjacent subcarriers. Hence, the received signals at the destination at even and odd subcarriers respectively are

$$y_D^k = \sqrt{E_{RD}}\, H_{RD}^k\, \hat{y}_R^k + \sqrt{E_{SD}}\, H_{SD}^k\, x_{k+1} + n_D^k \tag{3.4}$$

and

$$y_D^{k+1} = \sqrt{E_{SD}}\, H_{SD}^{k+1}\, x_k^* - \sqrt{E_{RD}}\, H_{RD}^{k+1}\, \hat{y}_R^{*k+1} + n_D^{k+1}, \tag{3.5}$$

where H_{RD}^k and H_{SD}^k are the channels response in frequency domain at subcarrier k for the links $R \to D$ and $S \to D$, respectively, $\hat{y}_R^k$ is the normalized signal from the relay at subcarrier k and n_D^k is AWGN with zero mean and variance σ_d^2. E_{SD} and E_{RD} are the energy of the links $S \to D$ and $R \to D$, respectively.

Hence, the matrix representation of the output of the Fast Fourier Transform (FFT) operation over a given SFBC is given by

$$\underbrace{\begin{bmatrix} y_D^k \\ y_D^{*\,k+1} \end{bmatrix}}_{\mathbf{y}_D} = \underbrace{\begin{bmatrix} \sqrt{\frac{E_{SR}\, E_{RD}}{E_{SR}+N_o}}\, H_{SRD}^k & \sqrt{E_{SD}}\, H_{SD}^k \\ \sqrt{E_{SD}}\, H_{SD}^{*\,k+1} & -\sqrt{\frac{E_{SR}\, E_{RD}}{E_{SR}+N_o}}\, H_{SRD}^{*\,k+1} \end{bmatrix}}_{\mathbf{H}} \mathbf{x} + \underbrace{\begin{bmatrix} \varphi_D^k \\ \varphi_D^{k+1} \end{bmatrix}}_{\boldsymbol{\varphi}_D}, \tag{3.6}$$

where $H_{SRD} = H_{RD}\, H_{SR}$, $\varphi_D^k = \sqrt{E_{RD}}\, H_{RD}^k\, n_R^k + n_D^k$.

To recover the transmitted signal, a matched filter (MF) receiver is used to acheive space diversity as follows

$$\hat{\mathbf{s}} = \mathbf{H}^H \mathbf{y}_D. \tag{3.7}$$

The output of the matched filter receiver can be expressed as follows

$$\hat{\mathbf{s}} = \mathbb{G}\bar{\mathbf{x}} + \tilde{\mathbf{n}}, \tag{3.8}$$

where $\hat{\mathbf{s}} = \begin{bmatrix} \hat{s}_k \\ \hat{s}_{k+1} \end{bmatrix}$ is the recovered signal and $\tilde{\mathbf{n}}$ is the decoded noise with zero mean and variance $\sigma^2_{\tilde{n}}$.

$\mathbb{G}$ in (3.8) can be expressed for two adjacent subcarriers k and $k+1$ as follows

$$\mathbb{G} = \begin{bmatrix} G_k & \varepsilon \\ \varepsilon^* & G_{k+1} \end{bmatrix}, \tag{3.9}$$

where $G_k = \sqrt{\frac{E_{SR}E_{RD}}{E_{SR}+N_o}} \left|H^k_{SRD}\right|^2 + \sqrt{E_{SD}} \left|H^{k+1}_{SD}\right|^2$, $G_{k+1} = \sqrt{E_{SD}} \left|H^k_{SD}\right|^2 + \sqrt{\frac{E_{SR}E_{RD}}{E_{SR}+N_o}} \left|H^{k+1}_{SRD}\right|^2$ are the diversity gains and ε and ε^* are the inter carrier interference (ICI) terms [50]. ε can be expressed as

$$\varepsilon = H^k_{SD}\, H^{*\,k}_{SRD} - H^{k+1}_{SD}\, H^{*\,k+1}_{SRD}. \tag{3.10}$$

The ICI terms, ε and ε^*, in (3.9) are a result of using the MF receiver and they are the source of the error floor in the BER performance.

3.3 Receiver Design

From (3.10), when the channel is constant over adjacent subcarriers, i.e., $H^k = H^{k+1}$, the error term (ε) will equal to zero. Hence, (3.9) will be diagonal.

$$\mathbb{G} = \begin{bmatrix} G_k & 0 \\ 0 & G_{k+1} \end{bmatrix}. \tag{3.11}$$

Nevertheless, in our case the channel is varying over adjacent subcarriers, i.e., ε is not equal to zero and $\mathbb{G}$ is not diagonal anymore. This causes ICI and consequently performance degradation. We propose a novel model to enhance the performance of the cooperative SFBC-OFDM system by eliminating the ICI terms and the error floor in the BER, caused by the MF receiver, while maintaining diversity gain. To solve this, we introduce a new receiver matrix, instead of the matrix $\mathbf{H}^H$ in (3.7), where the needed channel coefficients are compensated first before taking the conjugate transpose of the channel matrix. Therefore, the proposed channel matrix should satisfy the following condition

$$\mathbf{\Psi H} = \begin{bmatrix} G_k & 0 \\ 0 & G_{k+1} \end{bmatrix}, \tag{3.12}$$

where $\mathbf{\Psi}$ is the proposed receiver matrix.

To maintain the above condition (3.12), we write the channel matrix as

$$\mathbf{\Psi} = \begin{bmatrix} \frac{1}{U_k} & 0 \\ 0 & \frac{1}{U_{k+1}} \end{bmatrix} \mathbf{\Lambda}, \tag{3.13}$$

where U_k and U_{k+1} are the new diversity gains, $\mathbf{\Lambda}$ is as follows

$$\mathbf{\Lambda} = \begin{bmatrix} \sqrt{\frac{E_{SR}\,E_{RD}}{E_{SR}+N_o}}\; H_{RD}^{*\,k} H_{SR}^{*\,k} & \sqrt{E_{SD}}\; H_{SD}^{k+1}/A_k \\ \sqrt{E_{SD}}\; H_{SD}^{*\,k} & -\sqrt{\frac{E_{SR}\,E_{RD}}{E_{SR}+N_o}}\; H_{RD}^{k+1} H_{SR}^{k+1}/A_k^* \end{bmatrix} \tag{3.14}$$

and $A_k = K_{SRD}^* K_{SD}$, given that K_{SRD} and K_{SD} are the gain differences between channel coefficients of two adjacent subcarriers. K_{SRD} and K_{SD} are defined as

$$K_{SRD} = \frac{H_{SRD}^{k+1}}{H_{SRD}^{k}} \tag{3.15}$$

and

$$K_{SD} = \frac{H_{SD}^{k+1}}{H_{SD}^{k}}. \tag{3.16}$$

Hence, the diversity gains, U_k and U_{k+1}, can be expressed as

$$U_k = \sqrt{\frac{E_{SR}E_{RD}}{E_{SR}+N_o}} \left|H_{SRD}^{k}\right|^2 + \sqrt{E_{SD}} \left|H_{SD}^{k+1}\right|^2 / A_k \tag{3.17}$$

and

$$U_{k+1} = \sqrt{E_{SD}} \left|H_{SD}^{k}\right|^2 + \sqrt{\frac{E_{SR}E_{RD}}{E_{SR}+N_o}} \left|H_{SRD}^{k+1}\right|^2 / A_k^*. \tag{3.18}$$

By substituting the diversity gains U_k and U_{k+1} in (3.12), the proposed channel matrix $\mathbf{\Psi}$ satisfies the condition (3.12) and consequently the required receiver matrix is obtained.

3.4 Simulation Results

In this section, we present the simulation results of the proposed technique for a cooperative SFBC-OFDM system assuming number of subcarriers $N = 64$ per OFDM symbol block and a cyclic prefix (CP), $P = 16$. $S \to R$, $R \to D$ and $S \to D$ links are assumed to be frequency-selective multipath fading channels each of which consists of L multipath components. Assuming $S \to D$ and $R \to D$ links are balanced, i.e., $E_{SD} = E_{RD}$ and the transmitted data stream is chosen randomly from BPSK constellation with symbol rate $R_s = 4$ kbps.

In Fig. 3.2, we evaluate the BER performance of the proposed model with cooperative SFBC-OFDM system. Considering static frequency selective channels for the direct and relay assisted links, the numbers of multipath components are chosen as $L = 1$ and $L = 8$ for $S \to R$, $R \to D$ and $S \to D$ links. For $L = 8$ the normalized delay vector is $[0, 1, 2, 5, 7, 8]$ and the path gains are generated using jack's model as $[0.35, 0.28, 0.18, 0.13, 0.11, 0.09]$. According to the results given in Fig. 3.2, the proposed technique enhances the performance of the cooperative SFBC-OFDM system with high number of multipath components. At SNR = 12 dB, the proposed model can achieve a BER = 10^{-4}, while at the same SNR, the C-SFBC system performs approximately 10^{-3}. Moreover, the performance difference of the proposed model between $L = 1$ and $L = 8$ is 2.9 dB less than the performance difference of a cooperative SFBC-OFDM system with the same number of multipath components at BER = 2×10^{-3}.

Fig. 3.3 presents the BER performance of the proposed scheme for different values of Doppler frequency. Considering the normalized Doppler frequencies $F_d = 0.02$ and $F_d = 0.04$ which correspond to the Doppler frequencies $f_d = 100$ Hz and $f_d = 200$ Hz respectively, we notice that the proposed technique reduces the effect of the channel mobility. The normalized Doppler value F_d is evaluated using [37]

$$F_d = f_d T, \tag{3.19}$$

where T is the time duration of one OFDM symbol and is evaluated using

$$T = \frac{N}{N_a R_s}, \tag{3.20}$$

where N_a corresponds to number of OFDM symbols including the CP, i.e., $N_a = N + P$. For high SNR, the BER rate performance difference between static and mobile channels using the proposed method is less than the performance difference of cooperative SFBC-OFDM system. It is observed that the system performance at $f_d = 100$ Hz becomes closer to the system performance when the links $S \to R$, $R \to D$ and $S \to D$ are static. Hence, the proposed model mitigates the effect of the channel mobility and reduces the system degradation for high Doppler frequencies.

A comparison between the proposed model and STBC-OFDM system is performed for different Doppler frequencies. According to the results obtained from Fig. 3.4, we conclude that the proposed model enhances the cooperative SFBC-OFDM system versus cooperative STBC-OFDM system. For high SNR, the BER performance of the proposed scheme is much better than the BER performance of STBC-OFDM system considering the Doppler frequencies $f_d = 100$ Hz and $f_d = 200$ Hz. For Doppler frequency $f_d = 100$ Hz, the proposed model outperforms the C-STBC system by 4.6 dB at BER $= 2 \times 10^{-3}$.

In Fig. 3.5, we investigate the effect of the links $S \to R$, $R \to D$ and $S \to D$ at the performance of the proposed model. Fig. 3.5 shows that for high SNR, $R \to D$ link has the minimum effect to the performance. The system performance, when $R \to D$ link experiences higher Doppler frequency than the links $S \to R$ and $S \to D$, is close to the performance when all the links experience identical Doppler frequencies. On the other hand, $S \to R$ and $S \to D$ links have the same effect to the system performance. When the link $S \to R$ or $S \to D$ experiences higher Doppler frequency than the other links, the system performance of the proposed model becomes worse.

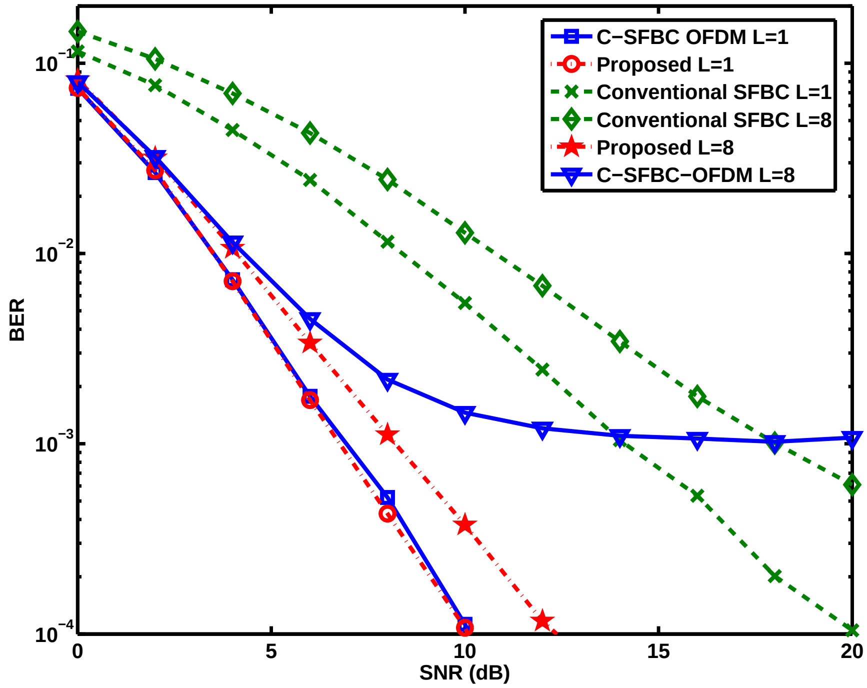

Figure 3.2: BER of cooperative system with different SNR values for S-R link

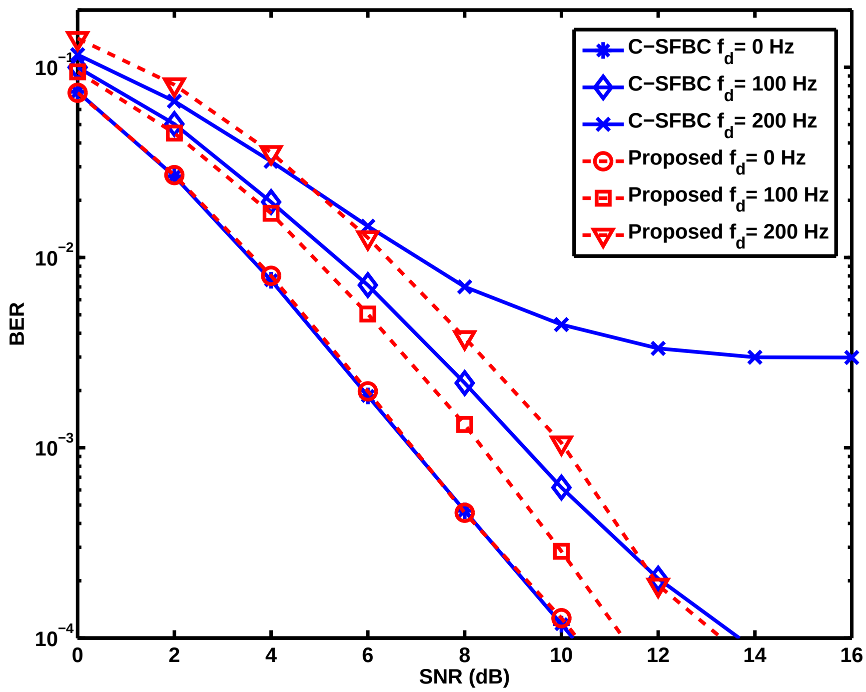

Figure 3.3: Proposed model performance at Doppler frequencies $f_d = 0$ Hz, $f_d = 100$ Hz and $f_d = 200$ Hz.

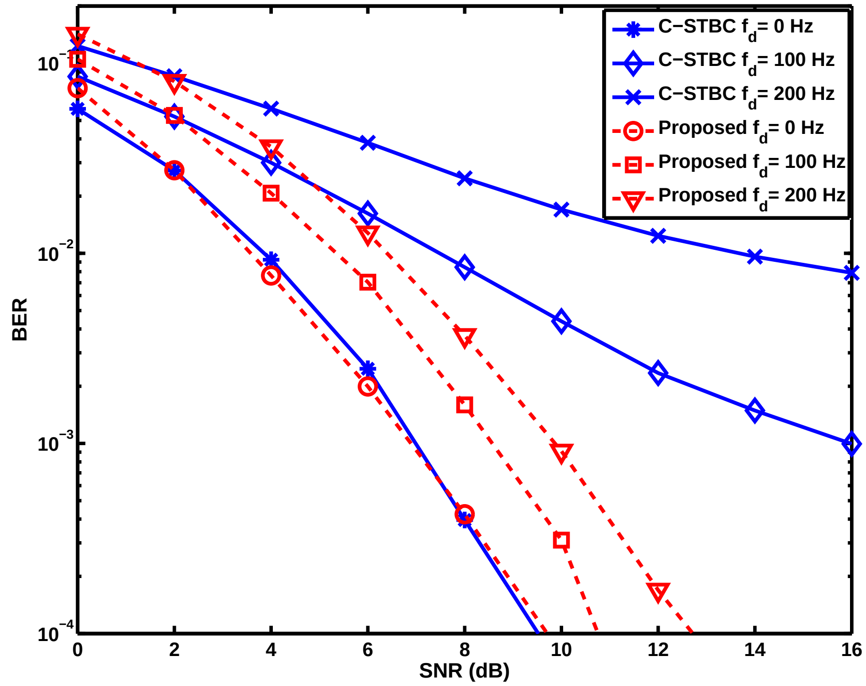

Figure 3.4: Performance comparison between the Proposed model and Cooperative STBC-OFDM system at Doppler frequencies $f_d = 0$ Hz, $f_d = 100$ Hz and $f_d = 200$ Hz.

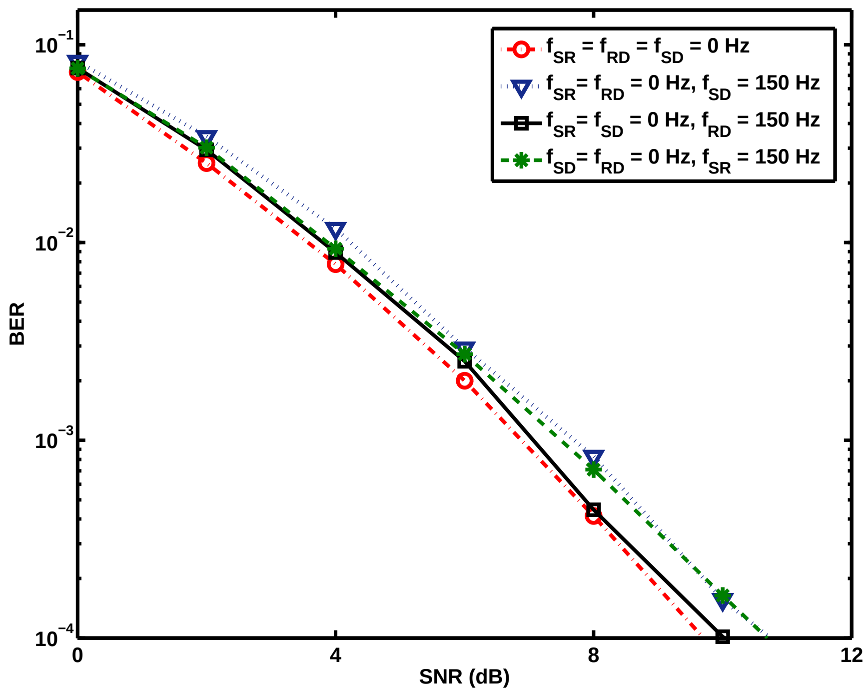

Figure 3.5: BER performance of the proposed model with different Doppler frequencies for the links $S \to R$, $R \to D$ and $S \to D$.

3.5 Conclusion

In this chapter, we have proposed a novel technique for a cooperative SFBC-OFDM system to enhance the BER performance by combating the effect of the time variation nature of the wireless channels. The proposed receiver aims to mitigate the ICI between the adjacent subcarriers and consequently mitigate the error floor on the BER performance. We have shown that the multipath cooperative SFBC system's reliability is improved using the proposed receiver. Also, we have showed that for higher number of multipath components, the system performance degradation for the proposed model is reduced compared to the cooperative SFBC system. In term of the Doppler frequency, we verified that the proposed model enhances the system BER performance even for high Doppler frequencies. We showed that the system becomes less susceptible to performance degradation for high Doppler frequencies. Finally, we showed that the $R \to D$ link has less affect to the system performance in comparison to $S \to R$ and $S \to D$ links.

Chapter 4

Optimal Precoder Design For AF MIMO Relay Networks with Antennas Selection

In this chapter, we introduce a source precoder design and sparse antenna selection technique with imperfect CSI. We assume the Amplify-and-Forward (AF) protocol in a single relay scenario equipped with multiple spatially correlated antennas.

4.1 Problem Statement

Cooperative MIMO systems have drawn considerable research efforts and various techniques have been introduced in recent years. Furthermore, there have been considerable research efforts on source and relay precoders to minimize the MSE in AF cooperative wireless systems [61–63]. For example, Tseng *et al.* [64] introduced the concept of joint source and relay precoders design by considering the direct and relay links for AF MIMO cooperative system. The proposed technique is based on diagonalizing the MSE matrix by deriving an analytical tractable MSE upper bound and use an iterative water-filling technique to obtain suboptimal solution for the precoders. Nevertheless, the proposed techniques in [61–64] assume perfectly known channels and spatially uncorrelated antennas at all nodes.

In summary, our goals in this chapters are:

- To provide a source precoder design with antenna selection technique by exploiting the sparsity of the relay gain vector.

- We consider practical scenarios by including imperfect CSI and spatially correlated antennas.

4.2 System Model

This work considers a cooperative wireless system composed of a source (S), a Relay (R) and a Destination (D), as shown in Fig. 4.1. The cooperative protocol III is adopted, where the transmitted symbols from the source to the destination pass through two phases. In the first phase, only the relay terminal receives the transmitted signal from the source. The destination terminal is silent during the first phase as it could be engaged in transmitting data to another terminal [43]. In the second phase, both the source and relay communicate with the destination over $S \rightarrow D$ and $R \rightarrow D$ links. We assume that the source, relay and destination terminals are equipped with N_T, M and N_R antennas, respectively. All links are modeled as flat fading channels. In this chapter, we consider cooperative MIMO system with spatially correlated antennas and imperfect CSI.

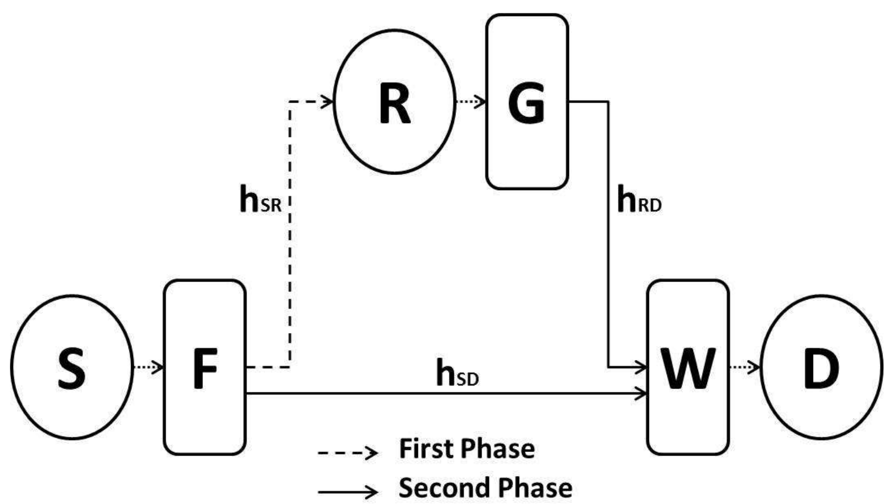

Figure 4.1: Cooperative AF MIMO system

4.2.1 Channel Correlation Model

The spatially correlated channel $\bar{\mathbf{H}}_{AB}$ between terminal A and B can be represented using the kroncker correlation model as follows [65]

$$\bar{\mathbf{H}}_{AB} = \boldsymbol{\Upsilon}_B^{1/2} \mathbf{H}_{AB} \boldsymbol{\Upsilon}_A^{1/2}, \tag{4.1}$$

where $\boldsymbol{\Upsilon}_B$ and $\boldsymbol{\Upsilon}_A$ are the antennas correlation matrices at terminals B and A, respectively, and $\mathbf{H}_{AB}$ is a random Gaussian channel matrix whose entries are independent and identically distributed with zero mean and unit variance. The spatial correlation matrices between the antennas at each node can be evaluated using the exponential model that is widely considered for constructing the correlation matrices as

$$\boldsymbol{\Upsilon}_{ij} = \begin{cases} \rho^{|j-i|}, & i \leq j \\ \left(\rho^{|j-i|}\right)^*, & i > j \end{cases}, \tag{4.2}$$

where ρ is a single correlation coefficient with $\rho \in \mathbb{R}$ and $|\rho| \leq 1$, i and j are the rows and columns of the correlation matrix $\boldsymbol{\Upsilon}$. It is worthnoting that the design is valid for any correlation matrix model, however, the results here were generated only for the exponential model. In our system, we consider three spatially correlated channels $\bar{\mathbf{H}}_{SR}, \bar{\mathbf{H}}_{RD}$ and $\bar{\mathbf{H}}_{SD}$ that represent the links between the three terminals $S \rightarrow R$, $R \rightarrow D$ and $S \rightarrow D$, respectively. $\bar{\mathbf{H}}_{SR}, \bar{\mathbf{H}}_{RD}$ and $\bar{\mathbf{H}}_{SD}$ can be rewritten as (4.1) as follows

$$\bar{\mathbf{H}}_{SR} = \boldsymbol{\Upsilon}_R^{1/2} \mathbf{H}_{SR} \boldsymbol{\Upsilon}_S^{1/2}, \tag{4.3}$$

$$\bar{\mathbf{H}}_{RD} = \boldsymbol{\Upsilon}_D^{1/2} \mathbf{H}_{RD} \boldsymbol{\Upsilon}_R^{1/2} \tag{4.4}$$

and

$$\bar{\mathbf{H}}_{SD} = \boldsymbol{\Upsilon}_D^{1/2} \mathbf{H}_{SD} \boldsymbol{\Upsilon}_S^{1/2}, \tag{4.5}$$

respectively, where $\boldsymbol{\Upsilon}_S$, $\boldsymbol{\Upsilon}_R$ and $\boldsymbol{\Upsilon}_D$ are $N_T \times N_T$, $M \times M$ and $N_R \times N_R$ correlation matrices at the source, the relay and the destination, respectively. $\mathbf{H}_{SR}$, $\mathbf{H}_{RD}$ and $\mathbf{H}_{SD}$ are random channels matrices whose entries are independent and identically distributed with zero mean and unit variance for the links $S \rightarrow R$, $R \rightarrow D$ and $S \rightarrow D$, respectively.

4.2.2 Imperfect Channel Estimation Modeling

Imperfect channel estimation is performed using the orthogonal training technique [66] to estimate the spatially correlated channels $\bar{\mathbf{H}}_{SR}$, $\bar{\mathbf{H}}_{RD}$ and $\bar{\mathbf{H}}_{SD}$. A training signal matrix $\mathbf{X}_t$ of size $N_T \times N_T$ is transmitted from the source and the received signal at the relay is

$$\mathbf{Y}_t = \boldsymbol{\Upsilon}_R^{1/2}\mathbf{H}_{SR}\boldsymbol{\Upsilon}_S^{1/2}\mathbf{X}_t + \mathbf{N}_t, \tag{4.6}$$

where $\mathbf{N}_t$ is additive white Gaussian noise matrix of size $M \times N_T$ with zero mean and variance σ_t^2. We choose the transmitted training signal to be $\mathbf{X}_t = \boldsymbol{\Upsilon}_S^{-1/2}\bar{\mathbf{X}}$, then

$$\mathbf{Y}_t = \boldsymbol{\Upsilon}_R^{1/2}\mathbf{H}_{SR}\boldsymbol{\Upsilon}_S^{1/2}\boldsymbol{\Upsilon}_S^{-1/2}\bar{\mathbf{X}} + \mathbf{N}_t. \tag{4.7}$$

To obtain the channel $\mathbf{H}_{SR}$, we pre-multiply the received training signal by $\boldsymbol{\Upsilon}_R^{-1/2}$ and post-multiply it by $\bar{\mathbf{X}}^{-1}$. Hence, we get the estimated channel $\tilde{\mathbf{H}}_{SR}$ as follow

$$\begin{aligned}\tilde{\mathbf{H}}_{SR} &= \boldsymbol{\Upsilon}_R^{-1/2}\mathbf{Y}_t\bar{\mathbf{X}}^{-1} \\ &= \mathbf{H}_{SR} + \underbrace{\boldsymbol{\Upsilon}_R^{-1/2}\mathbf{N}_t\bar{\mathbf{X}}^{-1}}_{\mathbf{E}_{SR}},\end{aligned} \tag{4.8}$$

where the total noise $\mathbf{E}_{SR}$ is AWGN with zero mean and variance σ_{noise}^2. Similarly, we can get the estimated channels $\tilde{\mathbf{H}}_{RD}$ and $\tilde{\mathbf{H}}_{SD}$ as follows

$$\begin{aligned}\tilde{\mathbf{H}}_{RD} &= \boldsymbol{\Upsilon}_D^{-1/2}\mathbf{Y}_t\bar{\mathbf{X}}^{-1} \\ &= \mathbf{H}_{RD} + \underbrace{\boldsymbol{\Upsilon}_D^{-1/2}\mathbf{N}_t\bar{\mathbf{X}}^{-1}}_{\mathbf{E}_{RD}}\end{aligned} \tag{4.9}$$

$$\begin{aligned}\tilde{\mathbf{H}}_{SD} &= \boldsymbol{\Upsilon}_D^{-1/2}\mathbf{Y}_t\bar{\mathbf{X}}^{-1} \\ &= \mathbf{H}_{SD} + \underbrace{\boldsymbol{\Upsilon}_D^{-1/2}\mathbf{N}_t\bar{\mathbf{X}}^{-1}}_{\mathbf{E}_{SD}},\end{aligned} \tag{4.10}$$

respectively, where $\mathbf{E}_{RD}$ and $\mathbf{E}_{SD}$ are the estimation error matrices.

4.2.3 Equalizer Model

Considering transmission protocol III, the received signal at the relay in the first phase with imperfect CSI is given by

$$\begin{aligned} \mathbf{y}_R &= (\mathbf{H}_{SR} + \mathbf{E}_{SR})\, \mathbb{F}_S \mathbf{x} + \mathbf{n}_1 \\ &= \mathbf{H}_{SR}\mathbb{F}_S\mathbf{x} + \underbrace{\mathbf{E}_{SR}\mathbb{F}_S\mathbf{x} + \mathbf{n}_1}, _{\mathbf{n}_R} \end{aligned} \tag{4.11}$$

where $\mathbb{F}_S$ is a $N_T \times n_T$ precoding matrix at the source, $\mathbf{x}$ is data vector to be transmitted from the source of size n_T, $\mathbf{n}_1$ is AWGN with distribution $\mathcal{N}\left(0, \sigma_{n_1}^2\right)$ and $\mathbf{n}_R$ is the total noise vector at the relay of size M with zero mean and variance σ_r^2. $\mathbf{H}_{SR}$ is $M \times N_T$ white gaussian channel with zero mean and unit variance. In the second transmission phase, the relay normalizes the received signal via the gain control matrix $\mathbf{G}$ and retransmits it to the destination. The received signal by the destination in the second phase is

$$\begin{aligned} \mathbf{y}_D &= (\mathbf{H}_{RD} + \mathbf{E}_{RD})\, \mathbf{G}\mathbf{y}_R + (\mathbf{H}_{SD} + \mathbf{E}_{SD})\, \mathbb{F}_S\mathbf{x} + \mathbf{n}_2 \\ &= \mathbf{H}_{RD}\mathbf{G}\mathbf{y}_R + \mathbf{H}_{SD}\mathbb{F}_S\mathbf{x} + \underbrace{\mathbf{E}_{RD}\mathbf{G}\mathbf{y}_R + \mathbf{E}_{SD}\mathbb{F}_S\mathbf{x} + \mathbf{n}_2,}_{\mathbf{n}_D} \end{aligned} \tag{4.12}$$

where $\mathbf{n}_2$ is additive white Gaussian noise vector of size N_R with zero mean and variance $\sigma_{n_2}^2$ and $\mathbf{n}_D$ is the total noise vector at the destination of size N_R with zero mean and variance σ_d^2. $\mathbf{H}_{RD}$ and $\mathbf{H}_{SD}$ are the $N_R \times M$ and $N_R \times N_T$ white Gaussian channels, respectively, with zero mean and unit variance.

The received signal in (4.12) can be expressed in a vector form as

$$\begin{aligned} \mathbf{y}_D = &\,[\, \underbrace{\mathbf{H}_{RD}\mathbf{G}\mathbf{H}_{SR}\mathbb{F}_S + \mathbf{H}_{SD}\mathbb{F}_S}_{\breve{\mathbf{H}}} \,]\, \mathbf{x} \\ &+ [\, \underbrace{\mathbf{H}_{RD}\mathbf{G}\mathbf{n}_R + \mathbf{E}_{RD}\mathbf{G}\mathbf{H}_{SR}\mathbb{F}_S\mathbf{x} + \mathbf{E}_{RD}\mathbf{G}\mathbf{n}_R + \mathbf{E}_{SD}\mathbb{F}_S\mathbf{x} + \mathbf{n}_2.}_{\mathbf{n}} \,] \end{aligned} \tag{4.13}$$

To recover the transmitted signal, an equalizer matrix $\mathbf{W}$ of size $n_T \times N_R$ is introduced. Using the MMSE criterion

$$\mathbf{MSE} = E\left[\|\mathbf{W}\mathbf{y}_D - \mathbf{x}\|^2\right], \tag{4.14}$$

the equalizer matrix $\mathbf{W}$ can be obtained as [64]

$$\mathbf{W} = \sigma_x^2 \breve{\mathbf{H}}^H \left(\sigma_x^2 \breve{\mathbf{H}} \breve{\mathbf{H}}^H + \mathbf{R}_w \right)^{-1}, \tag{4.15}$$

where σ_x^2 is the variance of the transmitted signal which assumed in our case to be one. $\mathbf{R}_w = E[\mathbf{w}\mathbf{w}^H]$ is the covariance matrix of the combined noise at the relay and the source with zero mean and variance σ_w^2. $\mathbf{R}_w$ can be expressed as

$$\mathbf{R}_w = \sigma_r^2 \mathbf{H}_{RD} \mathbf{G} \mathbf{G}^H \mathbf{H}_{RD}^H + \sigma_d^2 \mathbf{I}_M. \tag{4.16}$$

4.3 Precoder Design

In this section, the model introduced in [64] is adopted and modified for cooperative protocol III. Unlike the precoder design in [64], we are not considering a joint source/relay precoder design, since we are using antenna selection at the relay. Furthermore, our proposed precoder considers spatially correlated antennas and imperfect CSI to investigate the performance of the proposed model under realistic situations. The relay precoder is assumed to be identity matrix $\mathbf{F}_R = \mathbf{I}_M$. The optimization problem can be expressed as follows

$$\begin{cases} \underset{\mathbb{F}_S}{min} & \mathbf{MSE} \\ s.t. & \sigma_x^2\, tr\left\{\mathbb{F}_S \mathbb{F}_S^H\right\} \leq P_s \end{cases}, \tag{4.17}$$

where transmitted power at the source is $\mathbf{E}\left[\|\mathbb{F}_S \mathbf{x}\|^2\right] = \sigma_x^2\, tr\left\{\mathbb{F}_S \mathbb{F}_S^H\right\}$ and $\mathbf{MSE}$ is given in (4.28). To find the optimal source precoder, we consider the generalized singular value decomposition (GSVD) for the $S \rightarrow R$ and $S \rightarrow D$ channels to diagonalize the MSE matrix and SVD for $R \rightarrow D$ channel. The SVD of the $R \rightarrow D$ channel can be expressed as

$$\mathbf{H}_{RD} = \mathbf{U}_{RD} \mathbf{\Lambda}_{RD} \mathbf{V}_{RD}^H. \tag{4.18}$$

Also, The GSVD of the $S \rightarrow R$ and $S \rightarrow D$ links can be written, respectively, as

$$\mathbf{H}_{SR} = \mathbf{U}_{SR} \mathbf{\Lambda}_{SR} \mathbf{X}^H \tag{4.19}$$

and

$$\mathbf{H}_{SD} = \mathbf{U}_{SD}\mathbf{\Lambda}_{SD}\mathbf{X}^{H}. \tag{4.20}$$

From (4.27), considering the covariance matrix at the source $\mathbf{R}_{xx} = \mathbf{I}_{N_R}$,if we diagonalize $\mathbf{H}_{SD}\mathbb{F}_S\left(\mathbf{H}_{SD}\mathbb{F}_S\right)^H$, then the MSE matrix will be diagonalized. The given term can be rewritten, using the SVD of $\mathbf{H}_{SD}$, as

$$\mathbf{H}_{SD}\mathbb{F}_S\left(\mathbf{H}_{SD}\mathbb{F}_S\right)^H = \mathbf{U}_{SD}\mathbf{\Lambda}_{SD}\mathbf{X}^H\mathbb{F}_S\mathbb{F}_S^H\mathbf{X}\mathbf{\Lambda}_{SD}^H\mathbf{U}_{SD}^H. \tag{4.21}$$

We assumed that the relay precoder is an identity matrix $\mathbf{I}_M$. Hence, the term (4.21) can be diagonalized if the source precoder matrix is expressed as follows

$$\mathbb{F}_S = \mathbf{X}^{-H}\mathbf{\Lambda}_{SD}^{-1}\mathbf{U}_{SD}^{-1}\mathbf{\Lambda}_S, \tag{4.22}$$

where $\mathbf{\Lambda}_S$ is $N_T \times N_T$ diagonal matrix with diagonal elements $\lambda_s^i, i = 1, \cdots, N_T$. From (4.22), the power constraint at the source can be rewritten as

$$\sigma_x^2\, tr\left\{\mathbb{F}_S\mathbb{F}_S^H\right\} = \sigma_x^2 tr\left\{\mathbf{S}\mathbf{\Lambda}_S\mathbf{\Lambda}_S^H\right\}, \tag{4.23}$$

where $\mathbf{S} = \left(\mathbf{U}_{SD}\mathbf{\Lambda}_{SD}\mathbf{X}^H\mathbf{X}\mathbf{\Lambda}_{SD}\mathbf{U}_{SD}\right)^{-1}$ with diagonal elements $s_{ii}, i = 1, \cdots, N_T$. Considering $\alpha_i = \left(\lambda_s^i\right)^2$ and using the SVD and GSVD of the channels, the optimization problem in (4.17) can be expressed as follows

$$\begin{cases} \underset{\alpha_i}{min} & \sum_{i=1}^{N_T} \frac{1}{\sigma_x^{-2} + \frac{\left(\lambda_{rd}^i\lambda_{sr}^i\alpha_i + \lambda_{sd}^i\alpha_i\right)^2}{\sigma_r^2\lambda_{rd}^i + \sigma_d^2}} \\ s.t. & \sigma_x^2 \sum_{i=1}^{N_T} s_{ii}\alpha_i \le P_s \\ & \alpha_i \ge 0 \quad i = 1, \cdots, N_T \end{cases}, \tag{4.24}$$

where λ_{rd}^i, λ_{sr}^i and λ_{sd}^i are the ith diagonal elements of the matricess $\mathbf{\Lambda}_{RD}$, $\mathbf{\Lambda}_{SR}$ and $\mathbf{\Lambda}_{SD}$, respectively. Using Lagrange multiplier technique, the optimization problem in (4.24) can be expressed as

$$\alpha_i = \frac{N_T^3 s_{ii}^2 \sigma_x^2\left(\sigma_d^2 + \lambda_{rd}^i\,\sigma_r^2\right)}{\lambda_{sd}^i\,\sigma_x^{-2} + \lambda_{rd}^i\lambda_{sr}^i\,\sigma_x^{-2}\left(2\lambda_{sd}^i + \lambda_{rd}^i\lambda_{sr}^i\right) + N_T^2 s_{ii}^2\sigma_x^4\left(\sigma_d^2 + \lambda_{rd}^i\,\sigma_r^2\right)}. \tag{4.25}$$

In summary, our work differs from the work proposed in [64] in the way that our proposed precoder is derived while considering cooperative protocol III instead of protocol II where in cooperative protocol II the source transmits the data to the destination in addition to the relay in the first phase. In the second phase only the relay forwards the data to the destination. Moreover, spatially correlated antennas are considered at the three terminals and imperfect CSI is assumed for all links.

4.4 Antennas Selection with Gain Control

In this section, we present antenna selection technique for spatially correlated antennas with considering imperfect CSI. We introduce gain control matrix $\mathbf{G}$ at the relay terminal for MIMO system using the MSE criterion. Before using an equalizer, the error at the destination is

$$\mathbf{e} = \mathbf{x} - (\mathbf{H}_{RD}\mathbf{G}\mathbf{y}_R + \mathbf{H}_{SD}\mathbb{F}_S\mathbf{x} + \mathbf{n}_D). \tag{4.26}$$

To derive the MSE, first the error correlation matrix is expressed as follows

$$\begin{aligned} E\left[\mathbf{e}\mathbf{e}^H\right] = &\mathbf{R}_{xx} - \mathbf{H}_{RD}\mathbf{G}\mathbf{R}_{y_Rx} - \mathbf{H}_{SD}\mathbb{F}_S\mathbf{R}_{xx} \\ &- \mathbf{R}_{xy_R}\left(\mathbf{H}_{RD}\mathbf{G}\right)^H + \mathbf{H}_{RD}\mathbf{G}\mathbf{R}_{y_Ry_R}\left(\mathbf{H}_{RD}\mathbf{G}\right)^H \\ &+ \mathbf{H}_{SD}\mathbb{F}_S\mathbf{R}_{xy_R}\left(\mathbf{H}_{RD}\mathbf{G}\right)^H - \mathbf{R}_{xx}\left(\mathbf{H}_{SD}\mathbb{F}_S\right)^H \\ &+ \mathbf{H}_{RD}\mathbf{G}\mathbf{R}_{y_Rx}\left(\mathbf{H}_{SD}\mathbb{F}_S\right)^H \\ &+ \mathbf{H}_{SD}\mathbb{F}_S\mathbf{R}_{xx}\left(\mathbf{H}_{SD}\mathbb{F}_S\right)^H + \mathbf{R}_{n_Dn_D}, \end{aligned} \tag{4.27}$$

where

$$\begin{aligned} &\mathbf{R}_{xx} = E\left[\mathbf{x}\mathbf{x}^H\right] = \sigma_x^2\mathbf{I}_{N_T}, \\ &\mathbf{R}_{n_Dn_D} = E\left[\mathbf{n}_D\mathbf{n}_D^H\right] = \sigma_d^2\mathbf{I}_{N_R}, \\ &\mathbf{R}_{y_Ry_R} = E\left[\mathbf{y}_R\mathbf{y}_R^H\right] = \mathbf{H}_{SR}\mathbb{F}_S\mathbf{R}_{xx}\mathbb{F}_S^H\mathbf{H}_{SR}^H + \mathbf{R}_{n_Rn_R}, \\ &\mathbf{R}_{xy_R} = E\left[\mathbf{x}\mathbf{y}_R^H\right] = \mathbf{R}_{xx}\mathbb{F}_S^H\mathbf{H}_{SR}^H, \\ &\mathbf{R}_{y_Rx} = E\left[\mathbf{y}_R^H\mathbf{x}\right] = \mathbf{H}_{SR}\mathbb{F}_S\mathbf{R}_{xx}, \\ &\mathbf{R}_{n_Rn_R} = E\left[\mathbf{n}_R\mathbf{n}_R^H\right] = \sigma_r^2\mathbf{I}_M. \end{aligned}$$

The MSE in (4.27) can be expressed as

$$
\begin{aligned}
\mathbf{MSE} = \mathbf{tr}\Big\{&\mathbf{R}_{xx} - \mathbf{H}_{SD}\mathbb{F}_S\mathbf{R}_{xx} - \mathbf{R}_{xx}\left(\mathbf{H}_{SD}\mathbb{F}_S\right)^H \\
&+ \mathbf{H}_{SD}\mathbb{F}_S\mathbf{R}_{xx}\left(\mathbf{H}_{SD}\mathbb{F}_S\right)^H + \mathbf{R}_{n_D n_D} \\
&- \mathbf{R}_{xy_R}\mathbf{R}_{y_R y_R}^{-1}\mathbf{R}_{y_R x} + \mathbf{H}_{SD}\mathbb{F}_S\mathbf{R}_{xy_R}\mathbf{R}_{y_R y_R}^{-1}\mathbf{R}_{y_R x} \\
&+ \mathbf{R}_{xy_R}\mathbf{R}_{y_R y_R}^{-1}\mathbf{R}_{y_R x}\left(\mathbf{H}_{SD}\mathbb{F}_S\right)^H \\
&+ \mathbf{H}_{SD}\mathbb{F}_S\mathbf{R}_{xy_R}\mathbf{R}_{\mathbf{y}_R\mathbf{y}_R}^{-1}\mathbf{R}_{y_R x}\left(\mathbf{H}_{SD}\mathbb{F}_S\right)^H\Big\} \\
&+ \mathbf{tr}\left\{\left(\mathbf{H}_{RD}\mathbf{G} - \mathbf{R}_{xy_R}\mathbf{R}_{y_R y_R}^{-1}\right.\right. \\
&\left.+ \mathbf{H}_{SD}\mathbb{F}_S\mathbf{R}_{xy_R}\mathbf{R}_{y_R y_R}^{-1}\right)\mathbf{R}_{y_R y_R}\left(\mathbf{H}_{RD}\mathbf{G}\right. \\
&\left.\left.- \ \mathbf{R}_{xy_R}\mathbf{R}_{y_R y_R}^{-1} + \mathbf{H}_{SD}\mathbb{F}_S\mathbf{R}_{xy_R}\mathbf{R}_{y_R y_R}^{-1}\right)^H\right\}.
\end{aligned}
\tag{4.28}
$$

To find the optimum gain control matrix $\mathbf{G}$, we minimize the second term of (4.28) only, which will minimize the total MSE. Thus, the second term can be expressed, using the Cholesky factorization, as follows

$$
\begin{aligned}
&\mathbf{tr}\left\{\left(\mathbf{H}_{RD}\mathbf{G} - \mathbf{R}_{xy_R}\mathbf{R}_{y_R y_R}^{-1} + \mathbf{H}_{SD}\mathbb{F}_S\mathbf{R}_{xy_R}\mathbf{R}_{y_R y_R}^{-1}\right)\right. \\
&\left.\mathbf{L}_{y_R}\mathbf{L}_{y_R}^H\left(\mathbf{H}_{RD}\mathbf{G} - \mathbf{R}_{xy_R}\mathbf{R}_{y_R y_R}^{-1} + \mathbf{H}_{SD}\mathbb{F}_S\mathbf{R}_{xy_R}\mathbf{R}_{y_R y_R}^{-1}\right)^H\right. \\
&= \left\|\mathbf{H}_{RD}\mathbf{G} - \mathbf{R}_{xy_R}\mathbf{R}_{y_R y_R}^{-1} + \mathbf{H}_{SD}\mathbb{F}_S\mathbf{R}_{xy_R}\mathbf{R}_{y_R y_R}^{-1}\right\|_F^2,
\end{aligned}
\tag{4.29}
$$

where the positive-definite $\mathbf{R}_{y_R y_R} = \mathbf{L}_{y_R}\mathbf{L}_{y_R}^H$. Hence, minimizing MSE can be performed by minimizing $\mathbf{MSE}_F = \left\|\mathbf{H}_{RD}\mathbf{G} - \mathbf{R}_{xy_R}\mathbf{R}_{y_R y_R}^{-1} + \mathbf{H}_{SD}\mathbb{F}_S\mathbf{R}_{xy_R}\mathbf{R}_{y_R y_R}^{-1}\right\|_F^2$ which is controlled by the $N_R \times N_R$ gain control matrix $\mathbf{G}$. $\mathbf{MSE}_F$ can be rewritten in a vector form as

$$
\begin{aligned}
\mathbf{MSE}_F = \| &\underbrace{\left(\mathbf{I}_{N_R} \otimes \mathbf{H}_{RD}\right)}_{\ddot{\mathbf{H}}} . \underbrace{vec\left\{\mathbf{G}\right\}}_{\mathbf{g}_{N_R}} \\
&- vec\left\{\mathbf{R}_{xy_R}\mathbf{R}_{y_R y_R}^{-1} + \mathbf{H}_{SD}\mathbb{F}_S\mathbf{R}_{xy_R}\mathbf{R}_{y_R y_R}^{-1}\right\}\|_2^2 .
\end{aligned}
\tag{4.30}
$$

Antenna selection is performed by using Orthogonal Matching Pursuit (OMP) algorithm proposed in [67], which is a low complexity greedy algorithm that proved its efficiency in recovering sparse signals. The following is the used OMP formulation to minimize $\mathbf{MSE}_F$ by selecting antennas with antenna gain control.

$$
\begin{aligned}
\mathbf{g}_{N_R} = OMP\Big(&\ddot{\mathbf{H}}, vec\left\{\mathbf{R}_{xy_R}\mathbf{R}_{y_R y_R}^{-1} + \mathbf{H}_{SD}\mathbb{F}_S\mathbf{R}_{xy_R}\mathbf{R}_{y_R y_R}^{-1}\right\} \\
&, K_A \ \Big),
\end{aligned}
\tag{4.31}
$$

where K_A denotes the number of selected antennas, which is considered as the stopping criterion for the OMP algorithm. In (4.31), the OMP algorithm iteratively locates one locally optimum solution by solving one least square problem. The located solution at each iteration is considered as one optimum selection of the sparsely structured gain vector $\mathbf{g}_{N_R}$. Our proposed model for antenna selection is different from the model provided in [68] in that our model considers spatially correlated antennas at the three terminals in addition to imperfect CSI assumption, which is more realistic. Moreover, we are considering a direct link in addition to the relay link which enhances the system's reliability.

4.5 Benchmark Model

In this section, we provide a benchmark model for a joint source and relay precoders for the purpose of comparison and evaluation. The model in [64] considers both direct and relay links and aims to minimize the MSE to enhance the performance of AF cooperative MIMO system. The schematic representation of the system model in [64] is shown in Fig. 4.2. Protocol II is adopted where during the first time slot, both of the relay and destination listen to the source, while during the second time slot only the relay transmits to the destination. The received signal at the destination can be expressed in vector form as

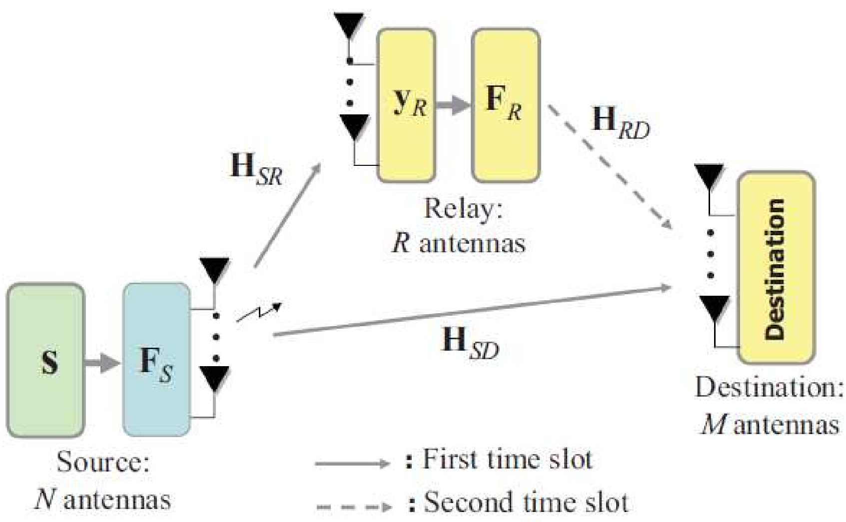

Figure 4.2: Schematic representation of model in [64]

$$\mathbf{y}_D = \underbrace{\begin{bmatrix} \mathbf{H}_{SD} F_S \\ \mathbf{H}_{RD}\mathbf{F}_R\mathbf{H}_{SR}\mathbf{F}_S \end{bmatrix}}_{\mathbf{H}} \mathbf{s} + \underbrace{\begin{bmatrix} \mathbf{n}_{D,1} \\ \mathbf{H}_{RD}\mathbf{F}_R\mathbf{n}_R + \mathbf{n}_{D,1} \end{bmatrix}}_{\mathbf{w}}, \tag{4.32}$$

where $\mathbf{H}_{SR} \in \mathbb{C}^{M\times N_T}, \mathbf{H}_{RD} \in \mathbb{C}^{N_R\times M}$, $\mathbf{H}_{SD} \in \mathbb{C}^{N_R\times N_T}$, $\mathbf{y}_D \in \mathbb{C}^{2N_R\times 1}$, $\mathbf{F}_S \in \mathbb{C}^{N_T\times n_T}$ and $\mathbf{F}_R \in \mathbb{C}^{M\times M}$. $\mathbf{n}_R \in \mathbb{C}^{M\times 1}$, $\mathbf{n}_{D,1} \in \mathbb{C}^{N_R\times 1}$ and $\mathbf{n}_{D,2} \in \mathbb{C}^{N_R\times 1}$ are the received noise vectors at the relay, at the destination at the first phase and the destination at the second phase, respectively.

The proposed technique in [64] is based on diagonalizing the MSE matrix by deriving an analytical tractable MSE upper bound and use an iterative water-filling technique to obtain suboptimal solutions for the precoders. The MMSE is derived by the authors as

$$J_{min} = tr\left\{\left(\sigma_s^{-2}\mathbf{I}_{n_T} + \mathbf{E}_S + \mathbf{E}_R\right)^{-1}\right\}, \tag{4.33}$$

with

$$\mathbf{E}_S = \sigma_{n,d}^{-2}\mathbf{F}_S^H\mathbf{H}_{SD}^H\mathbf{H}_{SD}\mathbf{F}_S \tag{4.34}$$

and

$$\mathbf{E}_R = \mathbf{F}_S^H\mathbf{H}_{SR}^H\mathbf{F}_R^H\mathbf{H}_{RD}^H\left(\sigma_{n,r}^2\mathbf{H}_{RD}\mathbf{F}_R\mathbf{F}_R^H\mathbf{H}_{RD}^H + \sigma_{n,d}^2\mathbf{I}_{N_R}\right)^{-1}\mathbf{H}_{RD}\mathbf{F}_R\mathbf{H}_{SR}\mathbf{F}_S. \tag{4.35}$$

To diagonalize the MSE matrix, the following optimization problem should be solved:

$$\begin{aligned}
&\underset{\mathbf{F}_S,\mathbf{F}_R}{min}\ tr\left\{\left(\sigma_s^{-2}\mathbf{I}_M + \mathbf{E}_S + \mathbf{E}_R\right)^{-1}\right\} \\
&s.t. \\
&tr\left\{E\left[\mathbf{F}_R\,\mathbf{y}_R\,\mathbf{y}_R^H\,\mathbf{F}_R^H\right]\right\} \le P_{R,T} \\
&tr\left\{\mathbf{F}_S E\left[\mathbf{s}\mathbf{s}^H\mathbf{F}_S^H\right]\right\} \le P_{S,T}.
\end{aligned} \tag{4.36}$$

Considering the SVD for all channels,

$$\begin{aligned}\mathbf{H}_{SD} &= \mathbf{U}_{SD}\Sigma_{SD}\mathbf{V}_{SD}^{H};\\ \mathbf{H}_{SR} &= \mathbf{U}_{SR}\Sigma_{SR}\mathbf{V}_{SR}^{H};\\ \mathbf{H}_{RD} &= \mathbf{U}_{RD}\Sigma_{RD}\mathbf{V}_{RD}^{H}.\end{aligned} \tag{4.37}$$

the optimization problem 4.36 can be solved by the following source and relay precoders:

$$\mathbf{F}_{S} = \mathbf{V}_{SR}\Sigma_{S} \tag{4.38}$$

and

$$\mathbf{F}_{R} = \mathbf{V}_{RD}\Sigma_{R}\mathbf{U}_{SR}^{H}, \tag{4.39}$$

respectively. A detailed derivations for the diagonal elements of the diagonal matrices Σ_S and Σ_R are provided in [64].

4.6 Simulation Results

In this section, we use a Monte-Carlo simulation to verify the results obtained previously in this chapter. We consider a MIMO system with number of antennas $N_T = M = N_R = 10$. The links $S \to R$, $R \to D$ and $S \to D$ are assumed to be flat fading channels and the transmitted data stream is chosen randomly from BPSK constellation with a symbol rate $R_s = 4$ kbps. For the antenna selection matrix, the number of the desired selected antennas is $K_A = 1$, to maintain the constraint of sparsity. We compare the BER performance of the proposed scheme with the BER performance of the technique introduced in [64], and the conventional AF technique, where the precoder is given by

$$\mathbb{F}_s = \sqrt{P_s/N}\,\mathbf{I} \tag{4.40}$$

$$\mathbb{F}_r = \sqrt{P_r/tr\left\{\mathbf{H}_{SR}\mathbb{F}_s\mathbb{F}_s^H\mathbf{H}_{SR}^H + \sigma_r^2\mathbf{I}\right\}}\,\mathbf{I} \tag{4.41}$$

Fig. 4.3 presents a comparison between the BER performance of the proposed model when we fix the relay links, $S \to R$ and $R \to D$, to 10 dB, the performance of the method proposed in [64] and the conventional method with correlation coefficient value $\rho = 0$. When we fix the SNR of the relay links and vary the SNR of the direct link from 0 to 10 dB, at low SNR, the performance of the proposed method is almost similar to the performance of the technique introduced in [64]. Nevertheless, at high SNR, the proposed model outperforms the method in [64]. At $SNR = 10$ dB, the performance of the proposed model is better than the performance of the method in [64] by 2.4×10^{-3} dB.

In Fig. 4.4 we fix the SNR value of the direct link to 10 dB and compare the BER performance of the proposed method and the two other methods considering uncorrelated antennas. From the figure, as the SNR of the relay links, $S \rightarrow R$ and $R \rightarrow D$, varies from 0 to 10 dB, we can see that the performance of the proposed method is highly better than the performance of the other two methods.

Spatially correlated antennas are considered in Fig. 4.5 with different correlation factor ρ. Even with correlated antennas, the proposed model outperforms the model in [64]. The performance of the proposed model is decreasing slowly while increasing the value of ρ. We consider correlation values $\rho = 0.3, \rho = 0.6$ and $\rho = 0.9$, we can observe that the performance of the proposed model is slightly changing while varying the correlation factor and even with considering highly correlated antennas for the proposed model, still it has better performance than the model in [64], where the antennas in [64] have low spatial correlation, relatively.

In Fig. 4.6, we evaluate the BER performance of the proposed model for different number of selected antennas K_A with setting the number of antennas at the relay $M = 50$. From the figure we can see that as we increase the number of selected antennas from 3 to 5 antennas, the performance suffers from small degradation. Hence, by exploiting sparsity of relay gain vector, the OMP aproach used in our proposed model let the system to achieve almost similarly for different number of antennas. Consequently, the proposed model reduces the complexity of the MIMO cooperative system and at the same time reduces the power consumption.

Fig. 4.7 represents the proposed model's performance with different variances for channel estimation error. From equations (4.8) and (4.9), we can see that as we increase the training signal, the estimation error decreases. From the results shown in Fig. 4.7, as expected, the performance of the systems suffers from degradation as we decrease the size of the training signal and this is stimulated by the increasing of the estimation error.

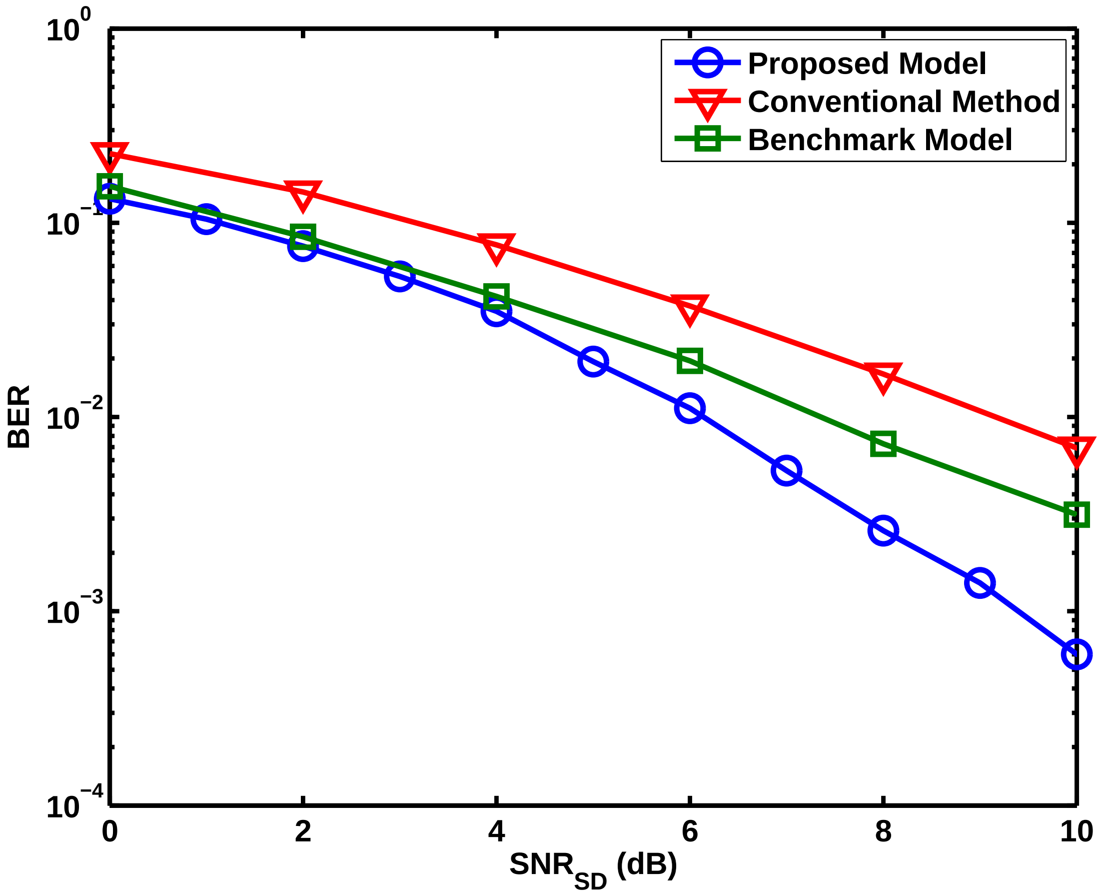

Figure 4.3: BER performance of the proposed model for fixed $S \rightarrow R$ and $R \rightarrow D$ links

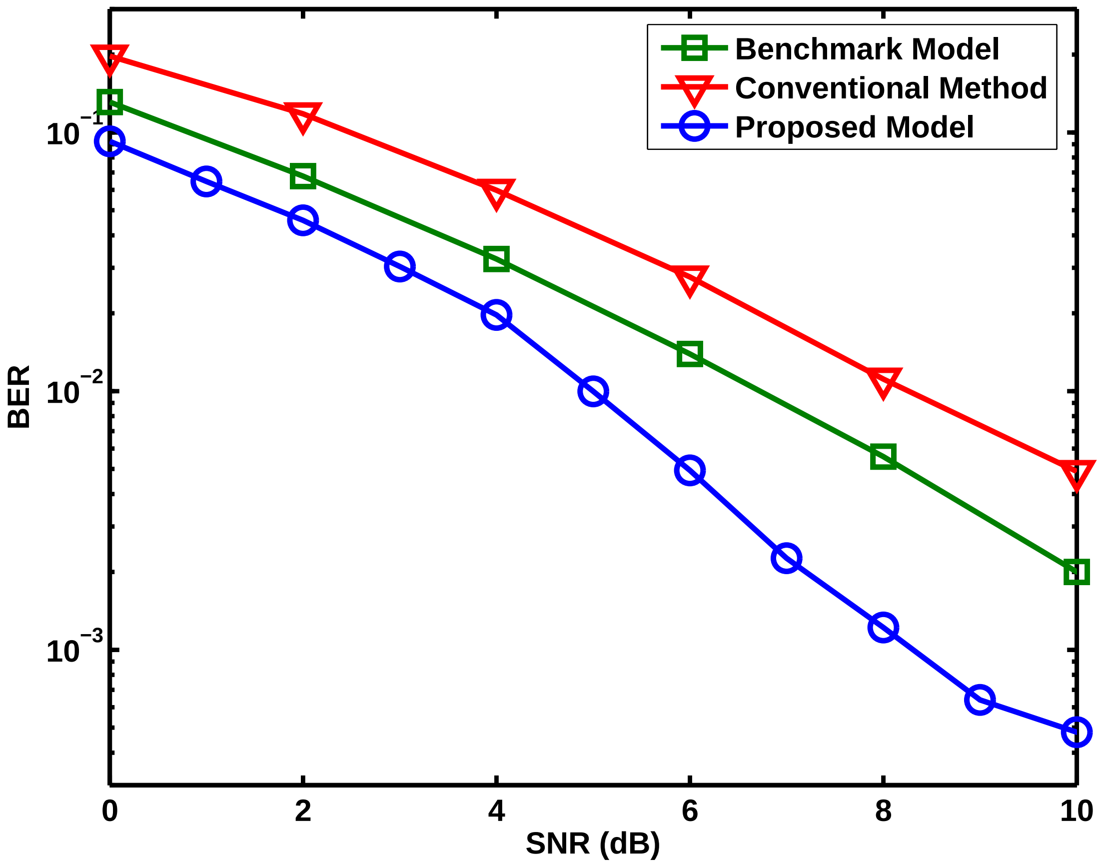

Figure 4.4: BER performance of the proposed model for fixed direct link

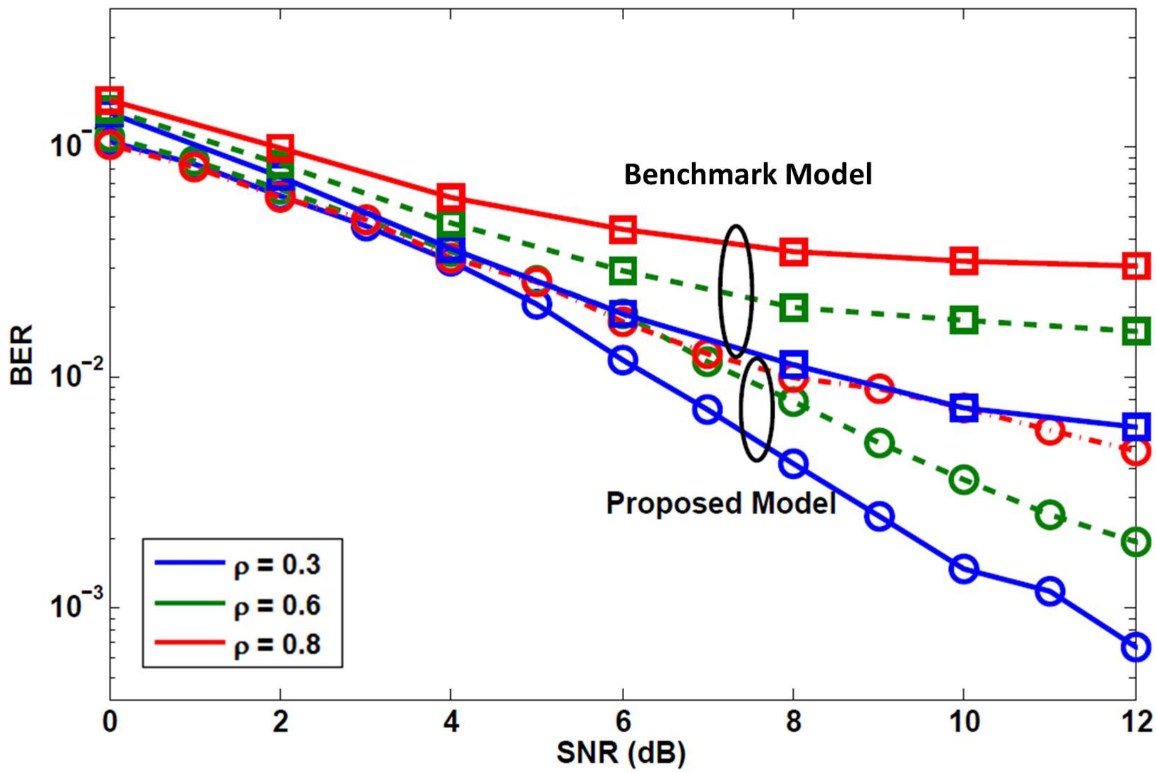

Figure 4.5: BER performance of the proposed model with different correlation factor

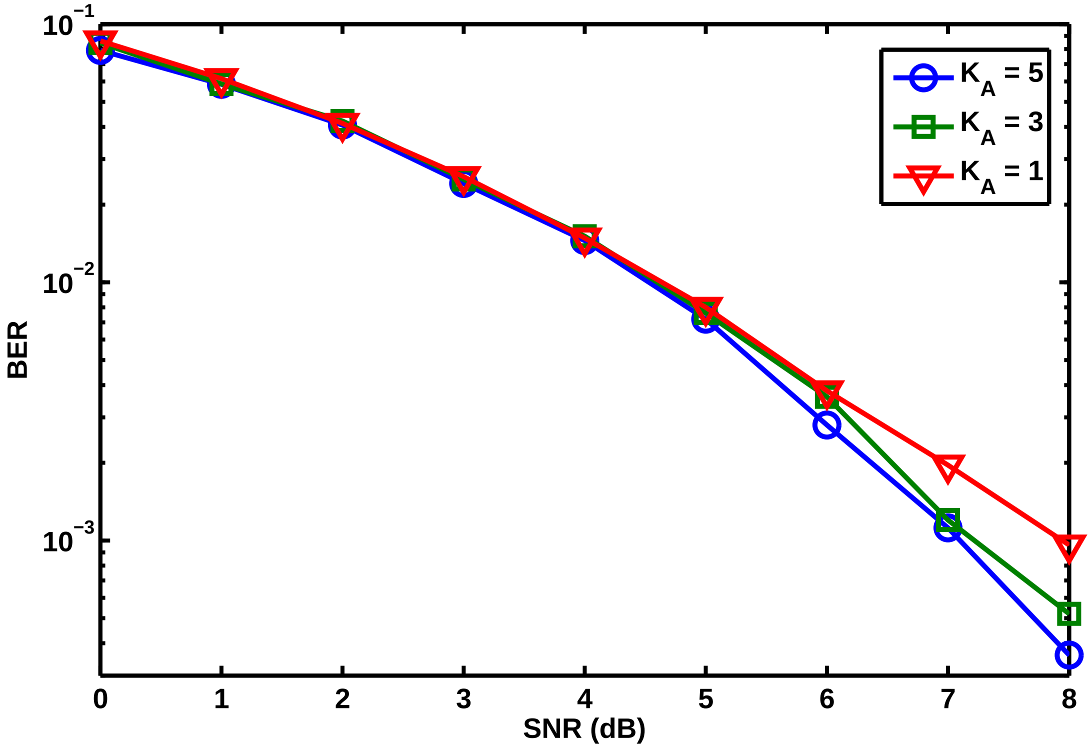

Figure 4.6: BER performance of the proposed model for different K_A values

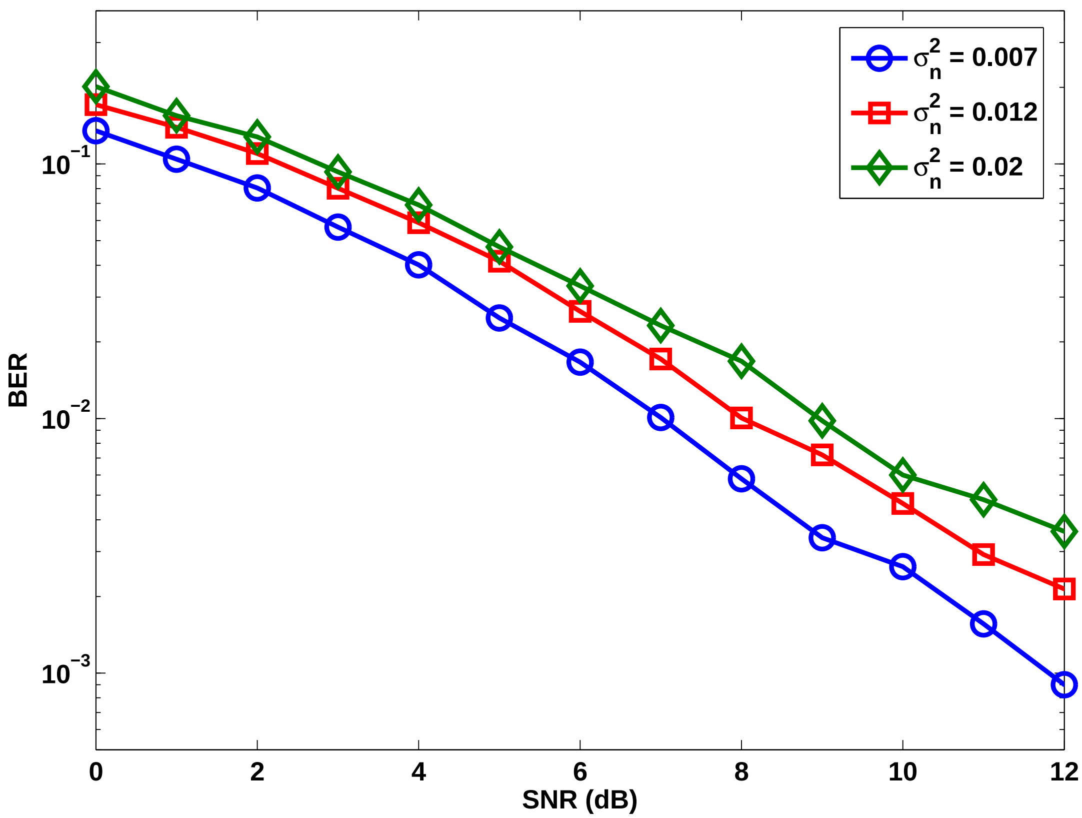

Figure 4.7: BER performance of the proposed model with different estimation errors

4.7 Conclusions

In this chapter, we have proposed an low efficient method to improve the performance of the MIMO cooperative system with spatially correlated antennas and imperfect CSI using the MMSE criterion. The proposed scheme consists of a source precoder and antenna selection at the relay. For the precoder, we adopt the SVD for the $R \to D$ and GSVD for $S \to R$ and $S \to D$ channels to design a precoder that normalizes the MSE matrix. Meanwhile, for the antenna selection technique, we use the OMP algorithm to generate the gain control matrix under the sparsity constraint. In our model, we considered imperfect CSI for all channels, the training algorithm is adopted for imperfect channel estimation. The simulation results for the proposed schemes showed that the proposed model enhances the system's performance for different SNR values for $S \to R$, $R \to D$ and $S \to D$. In term of number of selected antennas, we have showed that as we increase the number non-zero elements on the antenna selection matrix, the BER performance improved. Moreover, considering spatially correlated antennas, the proposed model outperforms the other models even for highly correlated antennas.

Chapter 5

Conclusions and Future Work

In this chapter, we conclude our thesis, highlight the main contributions, outline the limitations of this work and point out future work possibilities.

5.1 Conclusions

Cooperative communications exploits the broadcast nature of the wireless channels to deploy the overheard data by the neighboring nodes. However, time varying and frequency selective channels are considered among the main issues that face wireless channels.

In this research, we have presented two techniques for cooperative systems that aim to enhance the performance of the underlying system under different scenarios.

In Chapter 3, we have presented a new receiver design to improve the performance of SFBC-OFDM cooperative system by mitigating the ICI between the adjacent subcarriers. The main purpose of the proposed receiver is to combat the detrimental effect of doubly selective channels in a cooperative system. The design of the proposed receiver is based on compensating the channel gains to maintain the high diversity gain as the MF receiver. Moreover, the presented receiver avoids the matrix inversion of the classical ZF receivers. Simulation results are used to show the performance gain of the proposed system over the conventional cooperative SFBC-OFDM systems.

In Chapter 4, we have proposed a source precoder design for spatially correlated antennas at all terminals and imperfect CSI, to minimize the MSE of a MIMO cooperative system. Also, at the relay node we have presented antenna selection technique with antenna gain control based on the OMP algorithm. The well-known training method is adopted for imperfect channel estimation to assess the system's performance under realistic situations. Simulation results are provided to compare the performance of the proposed model with the existing models. The results show that for different correlation factors, the proposed method outperforms the other methods. Moreover, the proposed model's performance is evaluated with different estimation error variances.

5.2 Future Work

While this thesis has presented efficient techniques for improving the performance of cooperative systems, there are several possible research opportunities to extend the scope of this work. This section presents some of these possibilities.

In Chapter 3, we have proposed receiver design for AF cooperative SFBC-OFDM system with perfectly known channels. Hence, further extension to this work is to consider more practical scenarios such as imperfect CSI and to apply other relaying modes like the DF. Moreover, potential research extension is to consider the partial FFT (PFFT) instead of the FFT in the OFDM modulation.

In Chapter 4, extension to multiple relays scenarios is possible future work on the precoder design and relay antenna selection. Moreover, we will combine the OFDM technique with the existing techniques in the source precoder design and the antenna selection scheme. Doubly selective (frequency selective and time selective) channels will be considered with high Doppler frequencies values for the direct and the relay links to assess the performance of the proposed model on high mobility users.

Moreover, Performance and complexity analysis have not been done due to time limitation, so in future, both of the them will be performed for the proposed schemes.

5.3 List of Publications

Conference Papers:

- L. Bariah, S. Muhaidat and A. Al-Dweik, *Efficient SFBC-OFDM Technique for Broadband Cooperative Wireless Networks over Mobile channels.* The 15th IEEE International Workshop on Signal Processing Advances in Wireless Communications (SPAWC

2014).

Journal Papers:

- L. Bariah, S. Muhaidat and A. Al-Dweik, *Optimal Precoder Design for Non-regenerative MIMO Relay Networks with Antenna Selection*. Submitted for Publication.

Bibliography

[1] K. Jacobson and W. Krzymien, “System design and throughput analysis for multihop relaying in cellular systems,” *IEEE Trans. Veh. Technol.*, vol. 58, pp. 4514–4528, Oct 2009.

[2] V. Asghari, D. Benevides da Costa, and S. Aissa, “Performance analysis for multihop relaying channels with Nakagami-m fading: Ergodic capacity upper-bounds and outage probability,” *IEEE Trans. Commun.*, vol. 60, pp. 2761–2767, Oct 2012.

[3] Q. Cui, H. Wang, P. Hu, X. Tao, P. Zhang, J. Hamalainen, and L. Xia, “Evolution of limited-feedback CoMP systems from 4G to 5G: CoMP features and limited-feedback approaches,” *IEEE Veh. Technol. Mag.*, vol. 9, pp. 94–103, Sept 2014.

[4] C. Nie, P. Liu, T. Korakis, E. Erkip, and S. Panwar, “Cooperative relaying in next-generation mobile WiMAX networks,” *IEEE Trans. Veh. Technol.*, vol. 62, pp. 1399–1405, Mar 2013.

[5] J. Liu, N. Shroff, and H. Sherali, “Optimal power allocation in multi-relay MIMO cooperative networks: Theory and algorithms,” *IEEE J. Sel. Areas Commun.*, vol. 30, pp. 331–340, Feb 2012.

[6] H.-Y. Chen, J.-N. Lin, H.-S. Hu, and S.-J. Jou, “STBC-OFDM downlink baseband receiver for mobile WMAN,” *IEEE Trans. Very Large Scale Integr. (VLSI) Syst.*, vol. 21, pp. 43–54, Jan 2013.

[7] K. Lee, Y. Kim, and J. Kang, “A novel orthogonal space-time-frequency block code for OFDM systems,” *IEEE Commun. Lett.*, vol. 13, pp. 652–654, Sept 2009.

[8] U.-K. Kwon, G.-H. Im, and J.-B. Lim, “MIMO spatial multiplexing technique with transmit diversity,” *IEEE Signal Process. Lett.*, vol. 16, pp. 620–623, July 2009.

[9] L. Garcia-Ordonez, A. Pages-Zamora, and J. Fonollosa, "Diversity and multiplexing tradeoff of spatial multiplexing MIMO systems with CSI," *IEEE Trans. Info. Theory*, vol. 54, pp. 2959–2975, July 2008.

[10] C.-H. Liao, T.-P. Wang, and T.-D. Chiueh, "A 74.8 mW soft-output detector IC for 8 x 8 spatial-multiplexing MIMO communications," *IEEE J. Solid-State Circuits*, vol. 45, pp. 411–421, Feb 2010.

[11] C.-T. Lin and W.-R. Wu, "QRD-based antenna selection for ML detection of spatial multiplexing MIMO systems: Algorithms and applications," *IEEE Trans. Veh. Technol.*, vol. 60, pp. 3178–3191, Sept 2011.

[12] J. T. Wang, "Space-time coding with receive combiner bank for multiple-input-multiple-output system under multi-user cochannel interference," *IET Commun.*, vol. 7, pp. 180–186, Jan 2013.

[13] P. Luo and H. Leib, "Class of full-rank space-time codes combining orthogonal designs with delay diversity," *IEEE Trans. Veh. Technol.*, vol. 57, pp. 260–272, Jan 2008.

[14] L. Cao, M. Tao, and P. Kam, "Power control for MIMO diversity systems with non-identical rayleigh fading," *IEEE Trans. Veh. Technol.*, vol. 58, pp. 998–1003, Feb 2009.

[15] G. Amarasuriya, C. Tellambura, and M. Ardakani, "Multi-Way MIMO amplify-and-forward relay networks with Zero-Forcing transmission," *IEEE Trans. Commun.*, vol. 61, pp. 4847–4863, Dec 2013.

[16] A. Mehana and A. Nosratinia, "Diversity of MMSE MIMO receivers," *IEEE Trans. Info. Theory*, vol. 58, pp. 6788–6805, Nov 2012.

[17] J. Jalden and P. Elia, "DMT optimality of LR-Aided linear decoders for a general class of channels, lattice designs, and system models," *IEEE Trans. Info. Theory*, vol. 56, pp. 4765–4780, Oct 2010.

[18] X. Ge, X. Huang, Y. Wang, M. Chen, Q. Li, T. Han, and C. Wang, "Energy-efficiency optimization for MIMO-OFDM mobile multimedia communication systems with QoS constraints," *IEEE Trans. Veh. Technol.*, vol. 63, pp. 2127–2138, Jun 2014.

[19] G. Zhang, M. De Leenheer, A. Morea, and B. Mukherjee, "A survey on OFDM-based elastic core optical networking," *IEEE Commun. Surveys Tutorials*, pp. 65–87, 2013.

[20] R. Mesleh, H. Haas, S. Sinanovic, C. W. Ahn, and S. Yun, "Spatial modulation," *IEEE Trans. Veh. Technol.*, vol. 57, pp. 2228–2241, July 2008.

[21] R. Mesleh, H. Elgala, and H. Haas, "On the performance of different OFDM based optical wireless communication systems," *IEEE/OSA J. Opt. Commun. Networking*, vol. 3, pp. 620–628, Aug 2011.

[22] A. Al-Dweik, F. Kalbat, S. Muhaidat, O. Filio, and S. Ali, "Robust MIMO-OFDM system for frequency-selective mobile wireless channels," *IEEE Trans. Veh. Technol.*, vol. PP, no. 99, pp. 1–1, 2014.

[23] W.-L. Chin, "Blind symbol synchronization for OFDM systems using cyclic prefix in time-variant and long-echo fading channels," *IEEE Trans. Veh. Technol.*, vol. 61, pp. 185–195, Jan 2012.

[24] H.-Y. Chen, W.-K. Chang, and S.-J. Jou, "A low-overhead interference canceller for high-mobility STBC-OFDM systems," *IEEE Trans. Circuits Syst. I, Reg. Papers*, vol. 60, pp. 2763–2773, Oct 2013.

[25] S. Alamouti, "A simple transmit diversity technique for wireless communications," *IEEE J. Sel. Areas Commun.*, vol. 16, pp. 1451–1458, Oct 1998.

[26] X. Gao, W. Wang, X.-G. Xia, E. Au, and X. You, "Cyclic prefixed OQAM-OFDM and its application to single-carrier FDMA," *IEEE Trans. Commun.*, vol. 59, pp. 1467–1480, May 2011.

[27] T. Cooklev, H. Dogan, R. Cintra, and H. Yildiz, "A generalized prefix construction for OFDM systems over quasi-static channels," *IEEE Trans. Veh. Technol.*, vol. 60, pp. 3684–3693, Oct 2011.

[28] F. Fazel and H. Jafarkhani, "Quasi-orthogonal space-frequency and space-time-frequency block codes for MIMO OFDM channels," *IEEE Trans. Wireless Commun.*, vol. 7, pp. 184–192, Jan 2008.

[29] W. Martins and P. Diniz, "Block-based transceivers with minimum redundancy," *IEEE Trans. Signal Process.*, vol. 58, pp. 1321–1333, March 2010.

[30] H.-Y. Chen, M.-L. Ku, S.-J. Jou, and C.-C. Huang, "A robust channel estimator for high-mobility STBC-OFDM systems," *IEEE Trans. Circuits Syst. I, Reg. Papers*, vol. 57, pp. 925–936, Apr 2010.

[31] T. P. Ren, Y. L. Guan, C. Yuen, Y. Zhou, and E. Y. Zhang, "Optimization of fast-decodable full-rate STBC with non-vanishing determinants," *IEEE Trans. Commun.*, vol. 59, pp. 2063–2069, Aug 2011.

[32] R. Legnain, R. Hafez, and I. Marsland, “BER analysis of three-phase XOR-and-forward relaying using Alamouti STBC,” *IEEE Commun. Lett.*, vol. 16, pp. 1458–1461, Sept 2012.

[33] C. Yoon, H. Lee, and J. Kang, “Combined ML and DFE decoding for coded double STBC-OFDM system,” *IEEE Commun. Lett.*, vol. 14, pp. 1164–1166, Dec 2010.

[34] L. Xian and H. Liu, “Exact error probability for space-time block-coded MIMO systems over rayleigh fading channels,” *IEEE Proc.- Commun.*, vol. 152, pp. 197–201, Apr 2005.

[35] H. G. Ryu, “System design and analysis of MIMO SFBC CI-OFDM system against the nonlinear distortion and narrowband interference,” *IEEE Trans. Consum. Electron.*, vol. 54, pp. 368–375, May 2008.

[36] A. Abotabl, A. El-Keyi, Y. Mohasseb, and F. Bai, “Optimal windowing and decision feedback equalization for space x2013;frequency Alamouti-coded OFDM in doubly selective channels,” *IEEE Trans. Veh. Technol.*, vol. 63, pp. 2197–2207, Jun 2014.

[37] S. Lu, B. Narasimhan, and N. Al-Dhahir, “A novel SFBC-OFDM scheme for doubly selective channels,” *IEEE Trans. Veh. Technol.*, vol. 58, pp. 2573–2578, Jun 2009.

[38] M. Torabi, S. Aissa, and M. Soleymani, “On the BER performance of space-frequency block coded OFDM systems in fading MIMO channels,” *IEEE Trans. Wireless Commun.*, vol. 6, pp. 1366–1373, April 2007.

[39] D.-B. Lin, P.-H. Chiang, and H.-J. Li, “Performance analysis of two-branch transmit diversity block-coded OFDM systems in time-varying multipath rayleigh-fading channels,” *IEEE Trans. Veh. Technol.*, vol. 54, pp. 136–148, Jan 2005.

[40] A. Al-Dweik, A. Hazmi, S. Younis, B. Sharif, and C. Tsimenidis, “Carrier frequency offset estimation for OFDM systems over mobile radio channels,” *IEEE Trans. Veh. Technol.*, vol. 59, pp. 974–979, Feb 2010.

[41] Z. Mo, W. Su, S. Batalama, and J. Matyjas, “Cooperative communication protocol designs based on optimum power and time allocation,” *IEEE Trans. Wireless Commun.*, vol. 13, pp. 4283–4296, Aug 2014.

[42] R. Nabar, H. Bolcskei, and F. Kneubuhler, “Fading relay channels: performance limits and space-time signal design,” *IEEE J. Sel. Areas Commun.*, vol. 22, pp. 1099–1109, Aug 2004.

[43] H. Mheidat, M. Uysal, and N. Al-Dhahir, "Equalization techniques for distributed space-time block codes with amplify-and-forward relaying," *IEEE Trans. Signal Process.*, vol. 55, pp. 1839–1852, May 2007.

[44] O. Canpolat, M. Uysal, and M. Fareed, "Analysis and design of distributed space x2013;time trellis codes with amplify-and-forward relaying," *IEEE Trans. Veh. Technol.*, vol. 56, pp. 1649–1660, July 2007.

[45] A. Nasri, R. Schober, and I. Blake, "Performance and optimization of amplify-and-forward cooperative diversity systems in generic noise and interference," *IEEE Trans. Wireless Commun.*, vol. 10, pp. 1132–1143, April 2011.

[46] J. Kim, J. Lee, K. Son, S. Song, and S. Chong, "Two-hop opportunistic scheduling in cooperative cellular networks," *IEEE Trans. Veh. Technol.*, vol. 61, pp. 4194–4199, Nov 2012.

[47] X. Wu and L.-L. Xie, "On the optimal compressions in the compress-and-forward relay schemes," *IEEE Trans. Inf. Theory*, vol. 59, pp. 2613–2628, May 2013.

[48] D. Seol, U. Kwon, and G. Im, "Performance of single carrier transmission with cooperative diversity over fast fading channels," *IEEE Trans. Commun.*, vol. 57, pp. 2799–2807, Sep 2009.

[49] S. Yiu, D. Calin, O. Kaya, and K. Yang, "Distributed STBC-OFDM and distributed SFBC-OFDM for frequency-selective and time-varying channels," in *Wireless Communications and Networking Conference (WCNC)*, (Shanghai), pp. 251–255, 2012.

[50] B. Ozbek and D. Le Ruyet, "Low complexity ZF receiver for orthogonal SFBC-OFDM in broadband wireless channels," *Electronics Letters*, vol. 42, no. 8, pp. 479–481, 2006.

[51] A. Omri, R. Hamila, A. Hazmi, R. Bouallegue, and A. Al-Dweik, "Enhanced Alamouti decoding scheme for DVB-T2 systems in SFN channels," in *Personal Indoor and Mobile Radio Communications International Symposium (PIMRC)*, (Toronto), pp. 2046–2050, 2011.

[52] A. Al-Dweik, F. Kalbat, and S. Muhaidat, "Low complexity space-frequency MIMO-OFDM system for double-selective fading channels," *submitted to IEEE Trans. Veh. Technol.*

[53] H. Kyung and K. Kyung-Hwa, "An ICI suppression scheme based on the correlative coding for Alamouti SFBC-OFDM system with phase noise," *IEEE Trans. Wireless Commun.*, vol. 10, pp. 2023–2027, Jul 2011.

[54] K. Kwanghoon, P. Hyuncheo, and K. Hyuck, "Rate-compatible SFBC-OFDM under rapidly time-varying channels," *IEEE Trans. Commun.*, vol. 59, pp. 2070–2077, Aug 2011.

[55] Y. Yao and X. Dong, "Multiple CFO mitigation in amplify-and-forward cooperative OFDM transmission," *IEEE Trans. Commun.*, vol. 60, pp. 3844–3854, Dec 2012.

[56] H. Eghbali, S. Muhaidat, and N. Al-Dhahir, "A novel receiver design for single-carrier frequency domain equalization in broadband wireless networks with amplify-and-forward relaying," *IEEE Trans. Wireless Commun.*, vol. 10, pp. 721–727, Mar 2011.

[57] H. Mheidat and M. Uysal, "Equalization techniques for space-time coded cooperative systems," in *Vehicular Technology Conference (VTC)*, vol. 3, (Los Angeles), pp. 1708–1712 Vol. 3, 2004.

[58] A. Nasir, H. Mehrpouyan, S. Durrani, S. Blostein, R. Kennedy, and B. Ottersten, "Transceiver design for distributed STBC based AF cooperative networks in the presence of timing and frequency offsets," *IEEE Trans. Signal Process.*, vol. 61, pp. 3143–3158, Jun 2013.

[59] T.-T. Lu, H.-D. Lin, and T.-H. Sang, "An SFBC-OFDM receiver to combat multiple carrier frequency offsets in cooperative communications," in *Personal Indoor and Mobile Radio Communications Symposium (PIMRC)*, (Instanbul), pp. 899–904, 2010.

[60] J.-Y. Lee, H.-D. Lin, and T.-H. Sang, "An SFBC-OFDM receiver with MLSE equalizer to combat multiple frequency offsets," in *Circuits and Systems (ISCAS) Symposium*, (Seoul), pp. 1524–1527, 2012.

[61] R. Mo and W. Chew, "MMSE-based joint source and relay precoding design for amplify-and-forward MIMO relay networks," *IEEE Trans. Wireless Commun.*, vol. 8, pp. 4668–4676, Sept 2009.

[62] Y. Rong, "Optimal joint source and relay beamforming for MIMO relays with direct link," *IEEE Commun. Lett.*, vol. 14, pp. 390–392, May 2010.

[63] Y. Ding, J. Zhang, and K. Wong, "The amplify-and-forward Half-Duplex cooperative system: Pairwise error probability and precoder design," *IEEE Trans. Signal Process.*, vol. 55, pp. 605–617, Feb 2007.

[64] F. Tseng, W. Wu, and J. Wu, "Joint source/relay precoder design in nonregenerative cooperative systems using an MMSE criterion," *IEEE Trans. Wireless Commun.*, vol. 8, pp. 4928–4933, Oct 2009.

[65] S. Chatzinotas, M. Imran, and R. Hoshyar, "On the multicell processing capacity of the cellular MIMO uplink channel in correlated rayleigh fading environment," *IEEE Trans. Wireless Commun.*, vol. 8, pp. 3704–3715, July 2009.

[66] S. Serbetli and A. Yener, "MMSE transmitter design for correlated MIMO systems with imperfect channel estimates: power allocation trade-offs," *IEEE Trans. Wireless Commun.*, vol. 5, pp. 2295–2304, Aug 2006.

[67] J. Tropp and A. Gilbert, "Signal recovery from random measurements via orthogonal matching pursuit," *IEEE Trans. Inf. Theory*, vol. 53, pp. 4655–4666, Dec 2007.

[68] J. Lee and N. Al-Dhahir, "Exploiting sparsity for multiple relay selection with relay gain control in large AF relay networks," *IEEE Commun. Lett.*, vol. 2, pp. 347–350, June 2013.